

A sesquiterpene-rich essential oil from *Cannabis sativa* L. attenuates symptoms and neuroinflammation in experimental autoimmune encephalomyelitis model through a CB2-mediated signalling

Giacomina Videtta^a, Chiara Sasia^a, Sofia Quadrino^a, Virginia Brighenti^b, Laura Bertarini^{b,c}, Clarissa Caroli^{b,c}, Claudia Mugnaini^d, Federica Pellati^{b,**}, Nicoletta Galeotti^{a,*}

^a Department of Neurosciences, Psychology, Drug Research and Child Health (Neurofarba), Section of Pharmacology and Toxicology, University of Florence, Viale Gaetano Pieraccini 6, 50139 Florence, Italy

^b Department of Life Sciences, University of Modena and Reggio Emilia, Via Giuseppe Campi 103, 41125 Modena, Italy

^c Clinical and Experimental Medicine (CEM) PhD Program, University of Modena and Reggio Emilia, Via Giuseppe Campi 287, 41125 Modena, Italy

^d Department of Biotechnology, Chemistry and Pharmacy, University of Siena, via Aldo Moro 2, 53100 Siena, Italy

ARTICLE INFO

Keywords:

Cannabinoid receptors
Cannabis sativa
Demyelination
Essential oil
Multiple sclerosis
Pain

ABSTRACT

Background: The efficacy of cannabinoid-based medication as analgesic and neuroprotective in multiple sclerosis (MS) has been described, but little is known on other cannabis active compounds, such as terpenes.

Purpose: To investigate the therapeutic potential and molecular mechanism of non-psychoactive *Cannabis sativa* L. essential oil (EO) in an animal model of MS.

Methods: Chemical composition of EO was analyzed using GC-MS and GC-FID. Mouse model of experimental autoimmune encephalomyelitis (EAE) was employed to evaluate EO efficacy on pain (hot and cold plate test, von Frey test), motor disability (clinical score, rotarod), emotional alterations (sucrose splash test, tail suspension test, open field, light-dark box test) ($n = 11$). Tissues and LPS-stimulated BV2 cells were analyzed by Western blot, immunofluorescence, Luxol Fast Blue (LFB), hematoxylin and eosin (H&E) staining, UHPLC–HRMS analysis.

Results: β -caryophyllene, α -humulene, and caryophyllene oxide were the most abundant EO constituents. Intranasal administration of EO attenuated thermal and mechanical hypersensitivity, promoted motor function recovery, and induced antidepressant- and anxiolytic-like effects in EAE mice. EO increased LFB staining and MBP content while reducing H&E staining. In spinal cord and hippocampal tissues, EO reduced proinflammatory microglia (CD11b/IBA-1 ratio), restored the IL-17/IL-10 balance, and promoted a shift of microglia toward an anti-inflammatory phenotype by increasing CD206 and FoxP3 expression. Mechanistically, EO markedly upregulated CB2 receptor expression in both EAE mice and LPS-stimulated BV2 cells. The protective effect of EO was abolished by a CB2 antagonist (AM630) but not by CB1 blockade (AM251).

Conclusion: Intranasal EO alleviates EAE symptoms and comorbidities through a CB2-mediated attenuation of neuroinflammation and demyelination.

Abbreviations: 2-AG, 2-arachidonoylglycerol; AEA, anandamide; BCP, β -caryophyllene; CB1, cannabinoid receptor 1; CB2, cannabinoid receptor 2; CBD, cannabidiol; CFA, complete Freund's adjuvant; CNS, central nervous system; d.p.i., days post-immunization; EAE, experimental autoimmune encephalomyelitis; EO, Cannabis sativa L. essential oil; FoxP3, forkhead box P3; H&E, hematoxylin and eosin; LDB, light-dark box test; LFB, Luxol Fast Blue; LPS, lipopolysaccharide; MOG_{35–55}, myelin oligodendrocyte glycoprotein; MS, multiple sclerosis; OEA, oleoylethanolamide; OF, open field test; PEA, palmitoylethanolamide; RRMS, relapsing–remitting multiple sclerosis; SPMS, secondary progressive multiple sclerosis; SST, sucrose splash test; THC, Δ^9 -tetrahydrocannabinol; Treg, regulatory T cells; TST, tail suspension test.

* Corresponding author at: Department of Neurofarba, Viale Gaetano Pieraccini 6, 50139 Florence, Italy.

** Corresponding author at: Department of Life Sciences, Via Giuseppe Campi 103, 41125 Modena, Italy.

E-mail addresses: federica.pellati@unimore.it (F. Pellati), nicoletta.galeotti@unifi.it (N. Galeotti).

<https://doi.org/10.1016/j.phymed.2026.158068>

Received 20 October 2025; Received in revised form 2 March 2026; Accepted 9 March 2026

Available online 12 March 2026

0944-7113/© 2026 The Authors. Published by Elsevier GmbH. This is an open access article under the CC BY license (<http://creativecommons.org/licenses/by/4.0/>).

Introduction

Multiple sclerosis (MS) is a chronic autoimmune disease that affects the central nervous system (CNS), characterized by inflammation, demyelination gliosis and concomitant axonal loss (Ramaglia et al., 2021). Symptoms include fatigue, spasticity, alterations to vision, speech impairments, urinary bladder dysfunction, and severe weight loss (McGinley et al., 2021). Among MS symptoms, chronic pain is very frequent, affecting up to 87% of patients, that manifests as nociceptive or neuropathic pain, even at early disease stages. Neuropathic pain, that arises from nervous system damage, is one of the most debilitating symptoms with a prevalence among MS patients up to 58% (Rodrigues et al., 2023). Neuropsychiatric comorbidities, such as anxiety and depression, seriously affect the quality of life, disease progression, and overall outcome of patients (Rodrigues et al., 2023). The onset and intensity of clinical manifestations of MS depend on the site and severity of the lesions in the brain and spinal cord. Approximately 8590% of patients with MS present with a relapsing–remitting course of the disease (RRMS), and most of them advance to a progressive disease course, known as secondary progressive MS (SPMS), characterized by a gradual accumulation of disability (Jakimovski et al., 2024).

Remarkable progress has been made in the therapeutic development in MS, especially for RRMS (Gonzalez-Lorenzo et al., 2024). However, only one drug, ocrelizumab, is approved for primary progressive MS with a demonstrated decrease in disability progression (Riederer, 2017). Current therapies only partially protect against the continuous neurodegeneration that remains the major challenge. Recent advances suggest a central role for glial cells in the progressive disease process (Healy et al., 2022) and greater understanding of inflammation driven by CNS-resident cells is required to identify novel potential therapeutic opportunities. Evidence suggests that microglia play a pivotal role in both inflammation and remyelination processes (Guerrero and Scotte, 2020).

Studies on the use of medical cannabis in the treatment of MS suggest a reduction in pain and spasticity and most clinical trials have shown symptom improvement with cannabis-based drugs administration (Longoria et al., 2022). *Cannabis sativa* L. is, however, classified as a narcotic drug in many countries, mainly due to the presence of Δ^9 -tetrahydrocannabinol (Δ^9 -THC). In recent years, this view has been progressively revised as evidence has shown that the plant produces numerous phytochemicals with distinct pharmacological profiles, including non-psychoactive constituents lacking abuse potential (Odieka et al., 2022; Radwan et al., 2021). Consequently, efforts in the development of cannabis-based therapeutics have primarily focused on the major cannabinoids, Δ^9 -THC and the non-psychoactive cannabidiol (CBD) (Jones and Vlachou, 2020). However, undesirable central effects associated with cannabinoid receptor 1 (CB1) activation, including the worsening of cognitive functions already impaired in a significant proportion of MS patients, have limited the long-term use of CB1 agonists (Landrigan et al., 2022). This has fostered growing interest in non-cannabinoid components, such as terpenes.

Beyond phytocannabinoids (approximately 100 different compounds) considered the primary active components, more than 150 terpenes have been identified, representing the largest group of phytochemicals in *C. sativa* (Pieracci et al., 2021). Terpenes represent one of the largest groups of plant derived secondary metabolites and many of them are used as flavor ingredients and included in the Generally Recognized As Safe list (Adams et al., 2011). In contrast to the well-characterized cannabinoids, terpenes are primarily recognized for their ability to modulate cannabinoid-mediated responses (LaVigne et al., 2021). However, evidence has demonstrated that terpenes also exert biological activities independently of cannabinoids. Anti-inflammatory and antinociceptive effects have been described for the main cannabis terpenes (Liktov-Busa et al., 2021). However, only few studies have focused on the investigation of terpenes bioactivities, and their pharmacological properties in MS is still not elucidated.

The aim of the present study was to investigate the pharmacological activity of a sesquiterpene-rich essential oil (EO) obtained from inflorescences of a non-psychoactive *C. sativa* variety in relieving pain and associated comorbidities in an animal model of MS.

Materials and methods

Solvents and chemicals

Chromatographic grade solvents, including *n*-hexane, dichloromethane (DCM), acetonitrile (ACN), methanol (MeOH) and anhydrous sodium sulfate (Na_2SO_4) were purchased from Sigma-Aldrich (Milan, Italy). Reference standards of β -myrcene, limonene, linalool, β -caryophyllene, α -humulene, nerolidol and caryophyllene oxide (purity $\geq 98\%$) were from Sigma-Aldrich (Milan, Italy). Analytical standards for cannabinoids, namely cannabidiolic acid (CBDA), cannabigerolic acid (CBGA), cannabidiol (CBD) and cannabigerol (CBG), were purchased from Sigma Aldrich (Milan, Italy).

Water (H_2O) was purified using a Milli-Q® Advantage 10 system from Millipore (Milan, Italy).

Plant material

Cannabis sativa L. (hemp) inflorescences belonging to Kompolti variety, with a certified Δ^9 -THC content below 0.3%, was kindly provided by Materia Medica Processing (Siena, Italy). According to EU regulation, cannabis plants with a Δ^9 -THC content below 0.3% are considered as a non-narcotic and psychotropic (E.U. Regulation No 1307/2013 of the European Parliament).

Extraction of the essential oil from hemp inflorescences by means of steam distillation

Dried hemp inflorescences (120 g) were sieved to remove twigs and seeds and placed above the H_2O surface inside the steam-distillation apparatus. Once the temperature of 100 °C was reached in the system, the distillation was allowed to carry on for 2 h. The system was then let to cool to room temperature and hemp EO produced was separated from the scented H_2O and collected. To remove any trace of H_2O in the EO, it was dried with anhydrous Na_2SO_4 , which was removed by filtration on a paper filter. To reach the maximum yield of EO, the scented H_2O was washed three times with DCM in a separating funnel and the organic phase was then collected. The organic phase was finally dried under vacuum with a rotary evaporator and the residual oil was collected and combined with the EO previously obtained by distillation, thus providing a final yield of 0.12%.

Qualitative and semi-quantitative analysis of terpenes in the EO using GC–MS

The GC–MS analysis of the volatile compounds in the EO was performed on a 7820A gas chromatograph coupled with a 5975C network mass spectrometer (GC–MS) (Agilent Technologies, Waldbronn, Germany). Compounds were separated on an Agilent Technologies HP-5 MS cross-linked poly-5% diphenyl–95% dimethyl polysiloxane (30 m \times 0.32 mm inner diameter (i.d.), 0.25 μm film thickness) capillary column. The column temperature was initially set at 45 °C, then increased at a rate of 3 °C/min up to 170 °C, then raised to 200 °C at a rate of 6 °C/min, and again raised up to 280 °C at a rate of 13 °C/min, and finally held for 10 min. The injection volume was 1.5 μl , with a split ratio of 1:10. Helium was used as the carrier gas, at a flow rate of 1 ml/min. The injector, transfer line and ion-source temperatures were 250, 280 and 230 °C, respectively. MS detection was performed with electron ionization (EI) at 70 eV, operating in the full-scan acquisition mode in the *m/z* range 40–400. The EO was diluted 1:2000 (v/v) with *n*-hexane before GC–MS analysis.

The relative amount of volatile components was determined and expressed as percent relative peak area.

Quantitative analysis of main terpenes in the EO using GC-FID

The quantitative analysis of main volatile compounds in the EO was performed on a Shimadzu GC-2010 system coupled with a flame ionization detector (FID). The chromatographic column and the temperature program set for the GC-FID analyses were the same as those described in paragraph for the GC-MS analyses. The injector and detector temperature were set at 250 and 300 °C, respectively. Injection volume was 1.5 µl. Methyl octanoate was used as the internal standard (IS) for quantitative determination of terpenes. Hemp EO was diluted 1:2000 (v/v) with *n*-hexane and added of the IS solution prior the GC-FID analysis. Calibration curves for terpenes were constructed at five calibration levels in the range 5–80 µg/ml by plotting the ratio between the area of the analyte and that of the IS vs. their concentration ratio.

Analysis of cannabinoids in the EO using HPLC-UV

The analysis of cannabinoids in the EO was performed on an Agilent Technologies (Waldbronn, Germany) modular model 1260 Infinity II system, consisting of a quaternary pump, a manual injector and a UV variable wavelength detector. An Ascentis Express C₁₈ column (150 mm × 3.0 mm I.D., 2.7 µm, Supelco, Bellefonte, PA, USA) was used for the separation of target compounds, with a mobile phase composed of 0.1% HCOOH in both (A) H₂O and (B) ACN. The gradient elution was as follows: 0–13 min 60% B, 13–17 min from 60 to 80% B, 17–22 min from 80 to 90% B, which was kept for 8 min. The post-running time was 10 min. The flow rate was 0.4 ml/min. The sample injection volume was 3 µl. Chromatograms were acquired at 210 nm (for neutral cannabinoids) and at 220 nm (for cannabinoid acids) (Brighenti et al., 2017). The EO was diluted 1:2000 (v/v) with MeOH before HPLC-UV analysis. Calibration curves for target compounds were constructed at five calibration levels by plotting the peak areas of the analytes vs. their concentration.

Chromatograms were recorded by using an Agilent OpenLab ChemStation (Rev. C.01.10).

Endocannabinoid analysis

Endocannabinoid analysis on BV2 cell culture medium was performed by UHPLC–HRMS analysis. The detailed protocols used for sample preparation and analysis are described in the Supplementary Information.

Reagents and antibodies

The CB2 antagonist AM630 and the CB1 antagonist AM251 (Tocris, Bristol, UK) were dissolved in dimethyl sulfoxide. MOG_{35–55} peptide (synthesized by EspiKem Srl, University of Florence, Italy). Complete Freund's adjuvant (CFA), Luxol Fast Blue (LFB) (Sigma, Milan, Italy). Lipopolysaccharide (LPS) (Merck, Darmstadt, Germany). Primary antibodies: IBA-1 (#17198S), CD11b (#17800S), MBP (78896S), pERK1/2 (#4370S) pCREB (#9198S), CD206 (#24595S) (Cell Signaling Technology, Danvers, MA), CB2 (sc-293,188), IL-17 (sc-374,218), CD4 (sc-19,641), FoxP3 (sc-166,212), pNFκB (sc-136,548) (SantaCruz Biotechnology, Dallas, Texas), IL-10 (GTX632359), (GeneTex, Irvine, CA). Secondary antibodies labeled with Invitrogen Alexa 488 (#711–545–152) and 594 (#115–585–003) (Jackson ImmunoResearch Labs, West Grove, PA).

Animals

The EAE model was induced on C57BL/6 female mice (18–20 g, 6–8 weeks of age, Envigo, Varese, Italy). The animals were housed in the Ce. S.A.I. (Centro Stabulazione Animali da Laboratorio, University of

Florence), maintained at 23 ± 1 °C with a 12-hour light/dark cycle, light on at 7 a.m., fed by a standard laboratory diet and tap water ad libitum. Mice were left acclimatize for five days before testing. Cages were placed in the experimental room for 24 h before behavioral tests for acclimatization, and all tests were conducted during the light phase.

At the end of the experimentation mice were sacrificed by cervical dislocation for spinal cord and hippocampus removal for *in vitro* analysis. The number of animals for each experiment was based on a power analysis, and all groups tested included eleven animals.

Intranasal administration

Mice received a total of 10 µl of a solution containing 3 µg/mouse of EO, with 5 µl aliquots given into each nostril, as previously described (Borgonetti and Galeotti, 2021). Treatment was administered once daily starting from 14 days post-immunization (d.p.i.), when symptoms were well established. The dose of EO was chosen on the bases of dose-response curves (Fig. S1). Sham and MOG-EAE mice received vehicle i.n. on the same days.

EAE induction

The EAE model was induced by MOG_{35–55} peptide (Borgonetti and Galeotti, 2023a). Control mice (sham) received CFA without antigen. The general health, body weight, and disability score of all mice were monitored daily, locomotor coordination and noxious threshold were assessed before immunization and every three days thereafter until completion of the study. Mice were randomly assigned to 3 experimental groups: control (sham), immunized (MOG-EAE), immunized treated with EO. Control mice (sham) received CFA without antigen. All groups tested included eleven animals.

Behavioral testing

To assess the onset and progression of pain hypersensitivity and motor disability, the mice were monitored the day before immunization for baseline values and every 3 days thereafter until the end of the experimental model (Fig. 2A). All tests were performed under blinded conditions, with measurements collected by the same experimenter throughout the study.

von Frey's test

Mechanical threshold was measured by using von Frey monofilaments (Borgonetti and Galeotti, 2023b). Response was defined by paw withdrawal twice out of five completed stimuli.

Hot plate test

Thermal threshold was measured by using the hot-plate test (set at 52.0 °C). Licking or shaking of the paw or even jumping of the animal indicates reaction to the thermal stimulus; as soon as this response occurs, the counting of seconds to measure the reaction latency is stopped and the mouse is removed from the plate.

Rotarod test

The mouse locomotor coordination was measure by performing the rotarod test (Ugo Basile, Varese, Italy). Animals were placed on the rotating rod at the exact moment the stopwatch is operated. The integrity of the animal's motor coordination was assessed on the latency time from accelerating rotarod. The speed rotation progressively increases from 4 to 40 revolutions in 180 s.

Clinical disease score

A clinical disease score was assigned to each EAE and control mouse (sham) once daily in a blinded manner to assess the severity and extent of motor deficits. A disability scale ranging from 0 (no disability) to 5 (severe disability preceding the death of the animal) with half-point gradations was used (Borgonetti and Galeotti, 2023a). In any case, mice that reached a score of 3.5 were excluded from the study.

Open field test

Animals were positioned in the center of a box (78 × 60 × 39 cm) and the time each animal remained in the internal portion is measured, over a total duration of 5 min. The longer the animal stays in the center of the arena, the less anxious-like it is (Borgonetti and Galeotti, 2023b).

Light dark box test

Each mouse was allowed to move freely for 5 min in a box with two different compartments, the dark, and the light chamber, separated by a small door (10 cm × 3.2 cm), as previously described (Borgonetti and Galeotti, 2023b). The time spent in the light was used as a sign of the anxiety state of each animal.

Sucrose splash test

A 10% sucrose solution in H₂O was prepared and a small amount of this was placed on the animal back. The mouse was placed inside a box and the time spent cleaning in 5 min was measured (Borgonetti and Galeotti, 2023b).

Tail suspension test

Mice were suspended from a pole mounted 50 cm above the floor and the time during which the mice remained immobile was measured with a stopwatch (Borgonetti and Galeotti, 2023b). Immobility was considered a depression-like behavior (behavioral despair) and was measured in the first 2 min of the test, when the animals are reacting to unavoidable stress, and in the last 4 min, when behavioral despair is established.

Histopathology

Lumbar spinal cord sections (10 μm) were stained with Luxol Fast Blue (LFB) and with hematoxylin and eosin (H&E). The detailed protocols used is described in the Supplementary information.

BV2 cell culture and treatments

BV2 murine immortalized microglial cells (Tema Ricerca, Genova, Italy; 16–20 passages) were cultured in a medium containing RPMI with the addition of 10% of heat-inactivated (56 °C, 30 min) fetal bovine serum (FBS, Gibco, Milan, Italy) 1% glutamine, and a 1% penicillin–streptomycin solution at 37 °C in a 5% CO₂ humidified incubator. Cells were pretreated with AM630 or AM251 (1 μM) for 1 h and then treated with EO (0.01 - 0.1 - 1 μg/ml). After 4 h, to induce neuroinflammation, BV2 cells were stimulated for 24 h with LPS 250 ng/ml.

Sulforhodamine B (SRB) assay

Cells (2 × 10⁴ in 200 ml) were seeded in 96-well plates incubated with EO (0.01 - 0.1 - 1 μg/ml), fixed in 50% trichloroacetic acid at 4 °C for 1 h, treated with a solution of SRB 4 mg/ml in 1% acetic acid and incubated for 30 min at RT. Wells were washed four times with 1% acetic acid, added with 200 ml of TRIS HCl solution (pH=10) and incubated for 5 min with shaking. Absorbance was determined using a

microplate reader at 570 nm. Cell viability was calculated by normalizing the values to the mean of the control.

Cell counting and morphology

Cell counting and morphological analysis (quantification of total cell number, soma area and diameter) were performed by experimenter's blind to the cell culture conditions on images taken by Leica DM IL LED FLUO optical microscope and analyzed through the ImageJ program. Cells were counted per mm² microscopic area in at least ten randomly selected fields.

Western blot analysis

The lumbar spinal cord, hippocampus and BV2 cells lysates (20 μg) were separated on 10% SDS-PAGE and then blotted onto Midi Nitrocellulose membranes using a Trans-Blot Turbo Transfer Starter System (Biorad Laboratories, Milan, Italy). Blots were incubated overnight at 4 °C with specific antibodies, then, with horseradish peroxidase-conjugated secondary antisera (1:3000, Jackson ImmunoResearch Labs, West Grove, PA) for 2 h at RT. After washing, blots were developed using an enhanced chemiluminescence detection system (ChemiDoc Imaging Systems, Bio-Rad, Milan, Italy) and signal intensity (pixels/mm²) quantified (ImageJ 2.14, NIH, Bethesda, MD). Signal intensity was normalized against GAPDH.

Immunofluorescence

Lumbar spinal cord samples were fixed in formalin at 4% for 24 h, dehydrated in ethanol (EtOH), included in paraffin, and finally cut into 10 μm sections. BV2 cells were fixed with 4% PFA for 30 min at RT and cell membranes were permeabilized 0.1% PBS-tryton for up to five min. Membranes were blocked with BSA 5% in PBST and incubated with primary antibodies of interest overnight at +4 °C. After rinsing, the secondary antibodies were used at RT for 2 h. Sections were cover slipped using a Mounting Medium with DAPI. A Leica DM6000B fluorescence microscope equipped with a DFC350FX digital camera with appropriate excitation and emission filters for each fluorophore was used to acquire representative images. Images were acquired with 35 to 340 objectives using a digital camera. The immunofluorescence intensity was calculated using Image J 2.14.

Statistical analysis

Results are expressed as mean ± SEM. Repeated measures of two-way analysis of variance (ANOVA), followed by the Bonferroni test, were used to compare locomotor and nociceptive behaviors and mood parameters between immunized and sham mice. For biochemical and histological experiments, sample sizes subjected to statistical analysis had five samples per group ($n = 5$), where n is equal to the number of independent values. The level of significance was set to $p < 0.05$. Outliers were identified and excluded from each experimental set using the ROUT method (Motulsky and Brown, 2006). The computer program GraphPad Prism, version 10.3 (GraphPad Software Inc., San Diego, CA), was used.

Results

Chemical characterization of the EO

Volatile compounds in hemp EO were analyzed by both GC–MS and GC–FID. The identification of the compounds was achieved by comparing their MS spectral data and linear retention indexes (LRI) with those available in the literature and in the National Institute of Standards and Technology (NIST 14) mass spectral library. The results from the qualitative and semi-quantitative analysis of hemp essential oil are

shown in Table 1. GC–MS analysis allowed us to identify 44 compounds in hemp EO, encompassing monoterpenes, sesquiterpenes and cannabinoids.

The qualitative composition of hemp EO agreed with that described in the available literature (Iseppi et al., 2019; Janatová et al., 2022; Jin et al., 2021; Marini et al., 2018; Micalizzi et al., 2021; Pellati et al., 2018; Zheljzakov et al., 2025). Nevertheless, is it possible to observe that monoterpenes, which normally represent the major class of volatiles in the EO from *C. sativa*, together with sesquiterpenes, were poorly present in the sample analyzed (Iseppi et al., 2019; Janatová et al., 2022; Jin et al., 2021; Marini et al., 2018; Pellati et al., 2018). This fact could be attributable to the distillation process, in which a loss of monoterpenes, which are the most volatile compounds, may have occurred. According to the literature, β -myrcene is generally present in a relative percentage around 15–35% in this type of EO (Iseppi et al., 2019; Pellati et al., 2018; Vuerich et al., 2019), though in some cases the relative amount of β -myrcene was found to be lower than 5% (Iseppi et al., 2019; Janatová et al., 2022; Pellati et al., 2018; Pieracci et al., 2021; Xu et al., 2024).

Table 1

Semi-quantitative data of terpenes and cannabinoids in hemp EO, as determined by GC–MS. Data are expressed as percentage relative peak area (mean, $n = 3$) \pm SD.

Peak number	Compound	LRI	MW	% Peak area
1	Heptanal	903	114.19	< 0.1
2	β -Myrcene	994	136.23	0.1 ^a
3	Limonene	1028	136.23	0.1 ^a
4	1,8-Cineole (Eucalyptol)	1030	154.25	0.1 ^a
5	<i>trans</i> -Sabinene hydrate	1060	154.25	0.1 ^a
6	<i>cis</i> -Linalool oxide	1062	170.25	0.1 ^a
7	<i>cis</i> -Sabinene hydrate	1070	154.25	< 0.1
8	Linalool	1101	154.25	1.4 \pm 0.1
9	Fenchol	1113	154.25	0.2 ^a
10	<i>cis-p</i> -Mentha-2,8-dien-1-ol	1134	152.23	0.2 ^a
11	<i>trans</i> -Sabinol*	1136	152.23	0.2 ^a
12	Camphor	1144	152.23	0.3 ^a
13	Borneol	1164	154.25	0.8 ^a
14	Terpinen-4-ol	1177	154.25	0.4 ^a
15	<i>p</i> -Cymen-8-ol	1190	150.22	0.2 ^a
16	α -Terpineol	1191	154.25	0.6 \pm 0.1
17	Verbenone*	1204	150.22	< 0.1
18	Linalool formate*	1215	182.26	1.4 \pm 0.1
19	Geranyl acetate	1388	204.35	< 0.1
20	Ylangene	1389	204.35	0.4 ^a
21	Isocaryophyllene	1418	204.35	0.7 ^a
22	β -Caryophyllene	1425	204.35	31.5 \pm 0.6
23	α -Bergamotene	1439	204.35	0.8 ^a
24	α -Humulene	1459	204.35	10.6 \pm 0.1
25	Alloaromadendrene	1466	204.35	1.3 ^a
26	4,5-di-epi-Aristolochene*	1469	204.35	0.1 ^a
27	β -Selinene	1489	204.35	4.0 ^a
28	Valencene	1495	204.35	0.4 ^a
29	α -Selinene	1492	204.35	4.0 ^a
30	β -Bisabolene	1500	204.35	0.2 ^a
31	γ -Cadinene*	1525	204.35	1.7 ^a
32	δ -Cadinene	1527	204.35	0.4 ^a
33	γ -Selinene	1532	204.35	1.3 ^a
34	δ -Selinene	1545	204.35	2.9 ^a
35	Selina-3,7(11)-diene	1549	204.35	2.4 ^a
36	<i>trans</i> -Nerolidol	1567	222.37	2.6 \pm 0.1
37	Caryophyllene oxide	1591	220.35	7.3 \pm 0.2
38	Humulene-1,2-epoxide	1621	220.35	2.2 ^a
39	Selina-6-en-4-ol*	1624	222.37	1.5 \pm 0.1
40	Caryophylla-4(12),8(13)-dien-5-ol	1627	220.35	0.8 \pm 0.1
41	Germacre-4(15),5,10(14)-trien-1 α -ol*	1680	220.35	0.6 ^a
42	Juniper camphor	1709	222.37	0.5 ^a
43	Cannabicyclol (CBL)	2373	314.5	0.2 ^a
44	Cannabidiol (CBD)	2779	314.5	3.2 \pm 0.2

^a SD < 0.05.

* Tentatively identified with the NIST library.

Limonene and linalool were found in accordance with what is normally described in the literature, where they usually reach a percentage between 0–11% and 0–4%, respectively (Iseppi et al., 2019; Pellati et al., 2018; Pieracci et al., 2021). For what concern sesquiterpenes, β -caryophyllene (BCP) represents the most abundant compound in this EO, with a relative peak area slightly higher than what is described in the literature, where it normally ranges from 9 to 21% of the total peak area (Iseppi et al., 2019; Pellati et al., 2018; Pieracci et al., 2021; Zheljzakov et al., 2025). α -Humulene data were in accordance with the available literature, while caryophyllene oxide is present in a higher percentage in comparison to most samples described in the literature (Iseppi et al., 2019; Janatová et al., 2022; Jin et al., 2021; Marini et al., 2018; Pellati et al., 2018; Pieracci et al., 2021; Zheljzakov et al., 2025). The percentage peak area of CBD in hemp EO was much higher than what determined (Iseppi et al., 2019), but lower than what reported in a study by Pieracci et al. (2021). For what concerns cannabinoids, interestingly cannabicyclol (CBL) was detected in hemp EO. The presence of CBL in the EO can be considered as an artefact resulting from the degradation of other cannabinoids present in the plant material, such as cannabichromene (CBC) or cannabigerol (CBG), caused by long exposure to high temperature, both during the distillation process and the injection into the GC–MS injector port (250 °C) (Appendino et al., 2011; García-Valverde et al., 2022).

The main mono- and sesquiterpenes were quantified in hemp OE by means of GC-FID analysis. A representative GC-FID chromatogram is shown in Fig. 1, while Table 2 shows quantitative data.

The quantitative analysis of terpenes confirmed that sesquiterpenes were the predominant compounds in the EO, with BCP being the most abundant one, followed by α -humulene and caryophyllene oxide. Both BCP and α -humulene were found to be in a lower amount with respect to those determined by Joy et al. (2025), while nerolidol and β -caryophyllene oxide quantitative data were found to be comparable (Joy et al., 2025). As previously observed, monoterpenes were poorly represented in this EO: β -myrcene content was only 4.5 mg/ml detected in the EO, corresponding to 0.006 mg/g dry weight plant material, which is lower if compared to the available literature for hemp EO (5.9–8.6 mg of β -myrcene per g dry weight plant material) (Joy et al., 2025). Limonene content was under the limit of quantification (LOQ) value, while its content is described around 1.0 mg/g dry weight plant material (Joy et al. 2025), while linalool content agreed with the available literature (Joy et al., 2025).

To comprehensively characterize the content of secondary metabolites in hemp EO, the analysis of cannabinoids was carried out using HPLC-UV/Vis. A remarkable high amount of CBD was determined in the EO, when compared to the data available in the literature. Indeed, CBD content in hemp EO was found to be 60.9 \pm 0.3 mg/ml, against an average value in literature in the range 0.1–2.9 mg/ml (Iseppi et al., 2019).

Intranasal EO reduces nociceptive hypersensitivity in EAE mice

Hot thermal nociceptive hypersensitivity was produced in EAE mice from 3 dp.i. that progressively worsened peaking on day 21 pi. and remaining unaltered up to 28 dp.i. (Fig. 2B). Acute intranasal treatment with EO (14 dp.i.; Fig. 2C) as well as repeated treatment for 7 days (Fig. 2D) was ineffective. After 10-days treatment an increase of thermal threshold was observed (Fig. 2E) that was further increased after 14-days administration (Fig. 2F).

MOG_{35–55} immunization induced a drastic drop of cold thermal threshold from 7 dp.i. that persisted up to 28 dp.i. (Fig. 2G). No significant differences between untreated and EO-treated EAE animals were detected after acute (14 dp.i.; Fig. 2H) and 7-days repeated treatment (Fig. 2I). Ten-days administration showed a trend to an increase in the cold threshold (Fig. 2J) that become significant after a two-week treatment (Fig. 2K).

EAE showed mechanical allodynia from 3 dp.i. that peaked 18 dp.i.

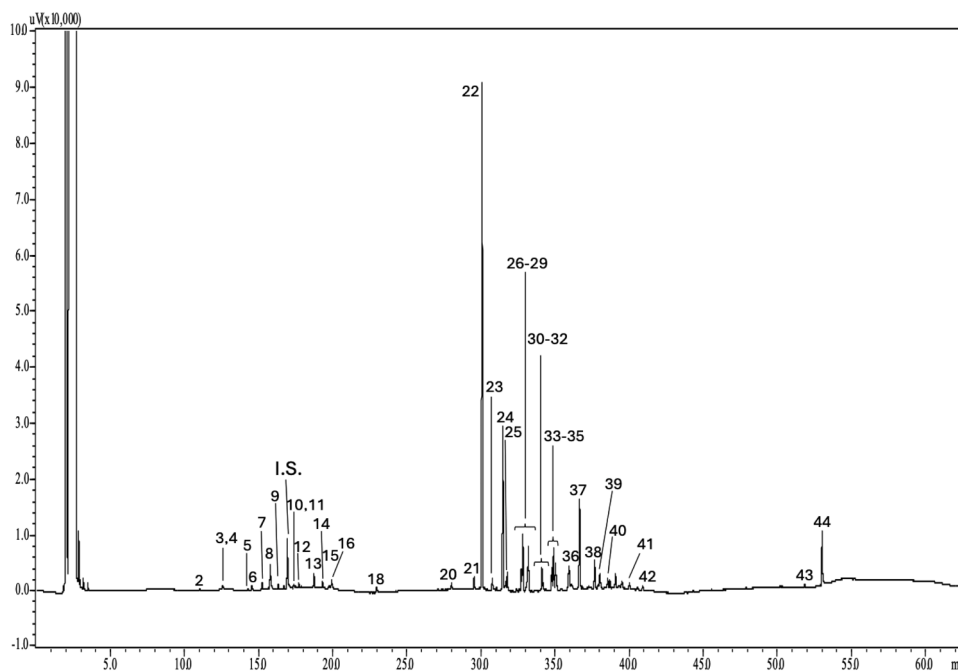


Fig. 1. GC-FID chromatogram of hemp EO. For peak identification, see Table 1.

Table 2

Quantification of main terpenes in hemp EO. Data are expressed as mg/ml (mean, $n = 3$) \pm SD.

Peak number	Compound	Content (mg/ml)
2	β -Myrcene	4.5 ^a
3	Limonene	< LOQ
8	Linalool	24.0 ^a
22	β -Caryophyllene	279.5 \pm 8.7
24	α -Humulene	145.6 \pm 1.9
36	Nerolidol	27.7 \pm 1.9
37	Caryophyllene oxide	84.2 \pm 4.7

^a SD < 0.05.

and remained unaltered up to 28 dp.i (Fig. 2I). Single (Fig. 2M) and 7-days repeated administration (Fig. 2N) of EO was ineffective. A trend towards an increase of mechanical threshold was observed 24 dp.i (Fig. 2O) while a significant effect was detected 28 dp.i. (Fig. 2P).

EO ameliorates motor symptoms in EAE mice

During the first week p.i., no significant differences in EAE clinical score and locomotor activity were observed between EAE and sham groups. At 10 dp.i. an increase of clinical score values was found in EAE mice that progressively worsened up to 28 dp.i. (Fig. 3B). A more detailed analysis of motor disability showed that EO repeated treatment significantly prolonged the time to onset (Fig. 3C) and the time to peak of disability (Fig. 3D), reduced the peak score values (Fig. 3E) and the cumulative score values (Fig. 3F).

A rotarod test was performed to investigate the locomotor coordination of EAE mice. Results showed a reduced endurance time on the rotating rod from 14 dp.i. that persisted up to 28 dp.i. (Fig. 3G). Acute (Fig. 3H) and repeated (Fig. 3H-K) intranasal administration of EO ameliorated the locomotor impairment by increasing the endurance time at all time points.

Lack of effect of EO on EAE-induced body weight loss

Control mice progressively increased their body weight over the 28-

day period of the study. Conversely, EAE mice starting from 14 dp.i. showed a lack of any body weight gain up to the end of experimentation (Fig. 3L). Although a trend toward some progressive weight gain by treatment over time, statistical significance was not reached (Fig. 3M-P).

EO protects EAE mice from depression-like and anxiety-like symptoms

The grooming time values in the sucrose splash test (SST) showed no difference between sham and EAE mice 14 (Fig. 4B) and 21 dp.i. (Fig. 4C), while 28 dp.i. a significant reduction of grooming time was detected in the EAE group (Fig. 4D). This effect was abolished by EO. To further investigate the antidepressant-like activity of the treatment, the Tail Suspension Test (TST) was performed 28 dp.i.; while not significant, EAE mice showed a trend towards an increase of the immobility time in the first 2 min of the test (Fig. 4E) and, to a lesser extent, in the last 4 min of the test when the behavioral despair is established (Fig. 4F). EO reduced the immobility time in the first 2 min (Fig. 4E), in the last 4 min (Fig. 4F) and the overall 6 min duration of the test (Fig. 4G).

The open field (OF) test showed a reduction of the time spent in the center 14 (Fig. 4H), 21 (Fig. 4I) and 28 dp.i. (Fig. 4J). EO administration at 14 (Fig. 4H) and 21 dp.i. (Fig. 4I) was ineffective, while, after a 2-week administration, there was a trend towards an increase of the time spent in the center (Fig. 4J). To verify the induction of an anxiolytic-like effect by EO, the light-dark box (LDB) test was performed 28 dp.i. EAE mice showed values for the time spent in the light chamber (Fig. 4K), number of transitions between the light and dark chambers (Fig. 4L) and latency values to the first step into the dark chamber (Fig. 4N) comparable to sham mice. However, EO increased the time spent in the light and the number of transitions, and reduced the latency to the first transition, showing an anxiolytic-like behavior.

EO protects EAE mice from spinal demyelination and inflammatory cell infiltration

Consistent with motor disability and nociceptive behavior, lumbar sections of spinal cords from EAE mice showed significant myelin loss, as indicated by a reduced LFB staining. In contrast, the frequency of demyelinating lesions was reduced in mice that received EO for 2 weeks (Fig. 5A,E). EAE mice also showed a trend towards a reduction of MBP

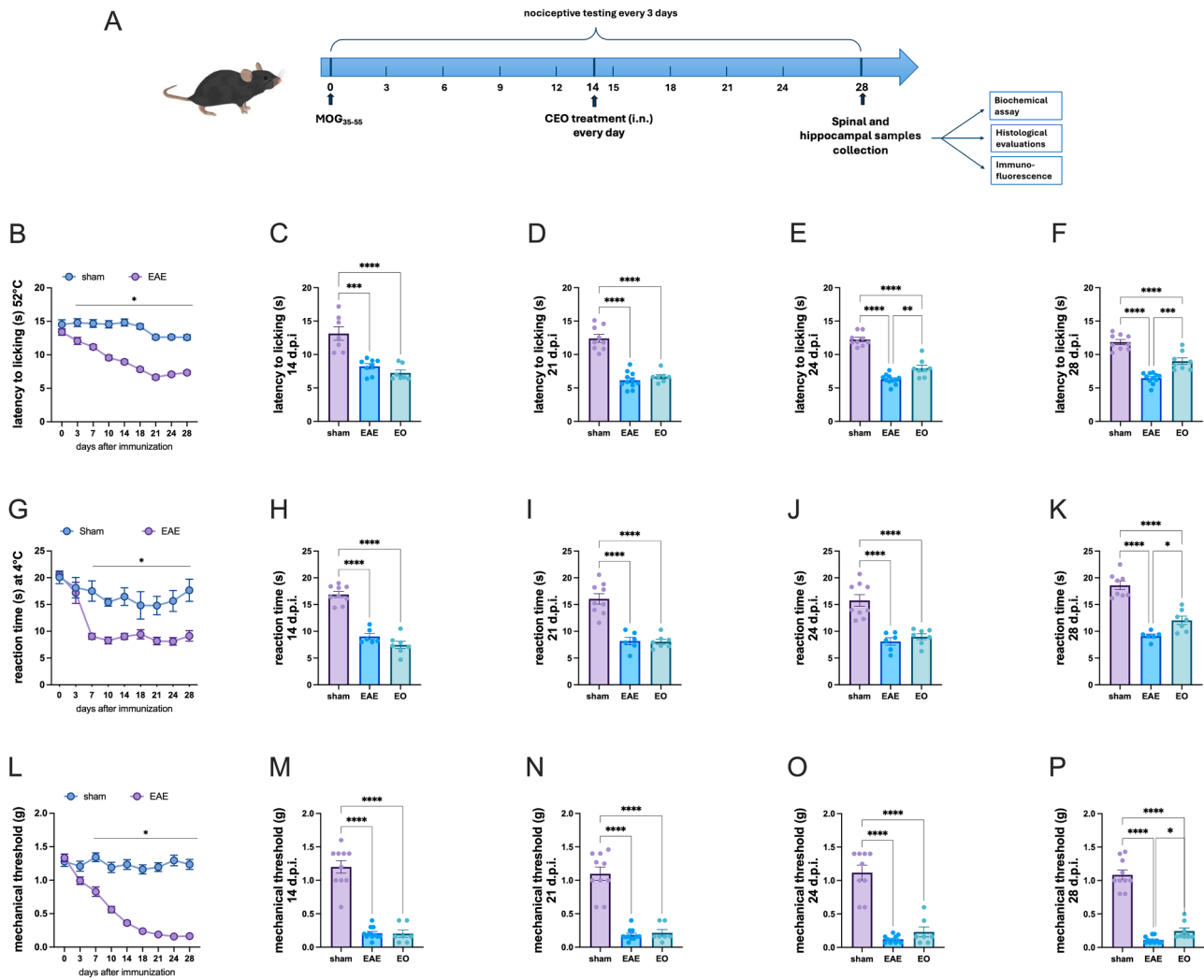


Fig. 2. EO attenuation of pain hypersensitivity in EAE mice.

(A) Schematic representation of the experimental protocol. (B) Time course evaluation of thermal hyperalgesia (hot stimulus, 52 °C) in EAE mice showing a progressive increase in pain hypersensitivity that peaked on 21 dp.i. Intranasal EO was not effective on 14 (C) and 21 dp.i. (D), whereas progressively alleviated thermal hypersensitivity on day 24 (E) and 28 dp.i. (F). (G) Determination of thermal threshold to a cold stimulus (4 °C) showed a drop in thermal sensitivity 7 dp.i. that remained unaltered up to the end of experimentation. Repeated intranasal administration of EO did not modify cold hyperalgesia 14 (H), 21 (I), and 24 (J) d.p.i. (K) A significant reduction of cold hypersensitivity was obtained 28 dp.i. (L) Time course study of mechanical allodynia in EAE mice showed a progressive decrease of mechanical threshold over time. EO was unable to attenuate mechanical hypersensitivity 14 (M), 21 (N) and 24 (O) d.p.i. while a significant effect was observed 28 dp.i. (P). EO was administered intranasally (3 µg/mouse i.n.) every day for two weeks starting from 14 dp.i.; Sham and MOG-EAE mice received vehicle i.n. on the same days. All groups tested included eleven animals. * $p < 0.05$, ** $p < 0.01$, *** $p < 0.001$, **** $p < 0.0001$.

protein levels that were robustly increased by EO (Fig. 5B).

Hematoxylin and Eosin (H&E) staining demonstrated pronounced lymphocytic infiltration (Fig. 5C) and elevated inflammatory scores (Fig. 5D) in the EAE group relative to sham controls, both of which were significantly mitigated by EO (Fig. 5C,D).

Attenuation of spinal neuroinflammation and microglia shift towards anti-inflammatory phenotype by EO

Immunofluorescence analysis (Fig. 5F) and protein quantification (Fig. 5G) revealed increased expression of IBA-1, a microglia marker, in the spinal cord of EAE mice compared with sham controls. Consistently, assessment of CD11b protein expression, a marker of activated microglia, showed a marked increase in the EAE group (Fig. 5H). EO further enhanced IBA-1 expression, while reduced CD11b levels. However, calculation of the CD11b/IBA-1 ratio demonstrated a clear increase in the EAE group, which was restored to basal levels by EO (Fig. 5I), indicating a counteracting effect on neuroinflammation. To investigate a

potential shift toward an anti-inflammatory microglia phenotype, the expression of IL-10, an anti-inflammatory cytokine, and IL-17, a proinflammatory cytokine, was examined. A trend toward increased IL-10 protein levels was observed in EAE mice, which was markedly potentiated by EO (Fig. 5J). Conversely, IL-17 protein levels were elevated in the EAE group and were not reduced by EO (Fig. 5K). Interestingly, calculation of the IL-17/IL-10 ratio showed a significant increase in EAE mice, which was normalized to basal levels by EO (Fig. 5L).

Following activation, CD4⁺ T cells can differentiate into either proinflammatory, mainly represented by Th17 which secrete IL-17 (Moser et al., 2020) or anti-inflammatory phenotypes, mainly represented by the immunosuppressive Treg (Knochelmann et al., 2018). An overall rise in CD4⁺ (Fig. 5M) and FoxP3⁺T cells (Fig. 5N) was observed in EAE mice, which was further enhanced by EO, suggesting a differentiation of CD4⁺ cells toward the Treg phenotype.

Finally, to assess the induction of a shift toward a microglia anti-inflammatory phenotype, the cellular localization and expression of the CB2 receptors was investigated. Immunofluorescence micrographs

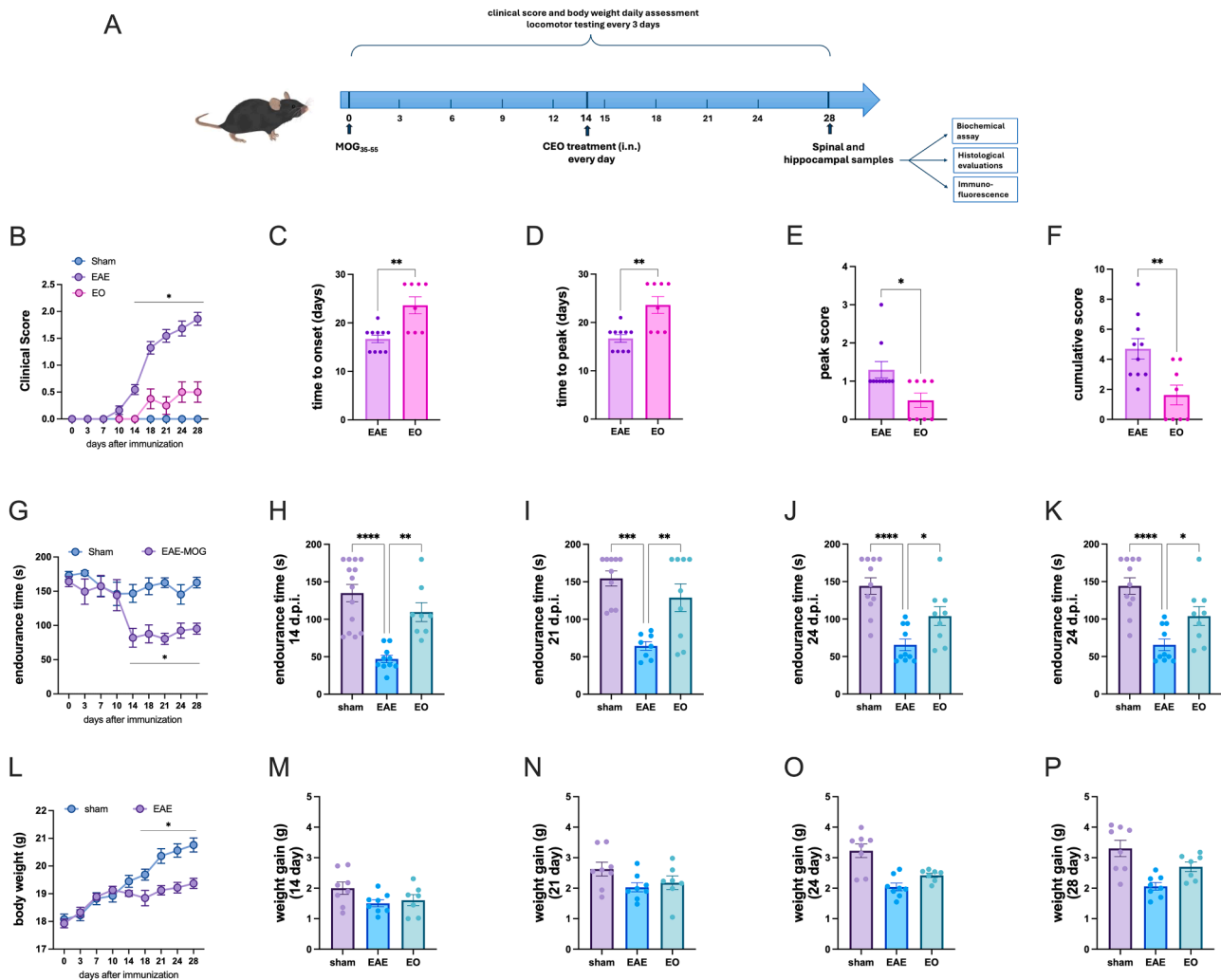


Fig. 3. Attenuation of motor symptoms by intranasal EO.

(A) Schematic representation of the experimental protocol. (B) Clinical disease score of MOG-EAE mice showed an increase of motor disability from 10 dp.i compared to sham mice. Attenuation by EO of disease clinical EAE score at all time points. EO treatment increased the time to onset (C) and time to peak (D) of disability and reduced the peak score (E) and cumulative score (F). $*p < 0.05$, $***p < 0.001$ versus sham mice (Wilcoxon test); $^{\circ\circ\circ}p < 0.01$ versus EAE mice (Kruskal–Wallis). (G) Progression of locomotor impairment in EAE mice by evaluating the rotarod performance time in comparison with sham mice. (H–K) Increase by EO of rotarod endurance time at all time point. EO was administered intranasally (3 $\mu\text{g}/\text{mouse}$ i.n.) every two days for two weeks starting from day 14 pi.; Sham and MOG-EAE mice received vehicle i.n. on the same days. $*p < 0.05$, $**p < 0.01$, $***p < 0.001$, $****p < 0.0001$. (L) Time course evaluation of body weight in EAE mice showed a lack of progressive increase over time by EAE mice starting from 14 dp.i.. EAE mice showed a reduced body weight gain 14 (M), 21 (N), 24 (O) and 28 dp.i. (P). EO administered intranasally (3 $\mu\text{g}/\text{mouse}$ i.n.) did not produce any significant effect. All groups tested included eleven animals. $*p < 0.05$, $**p < 0.01$, $***p < 0.001$, $****p < 0.0001$.

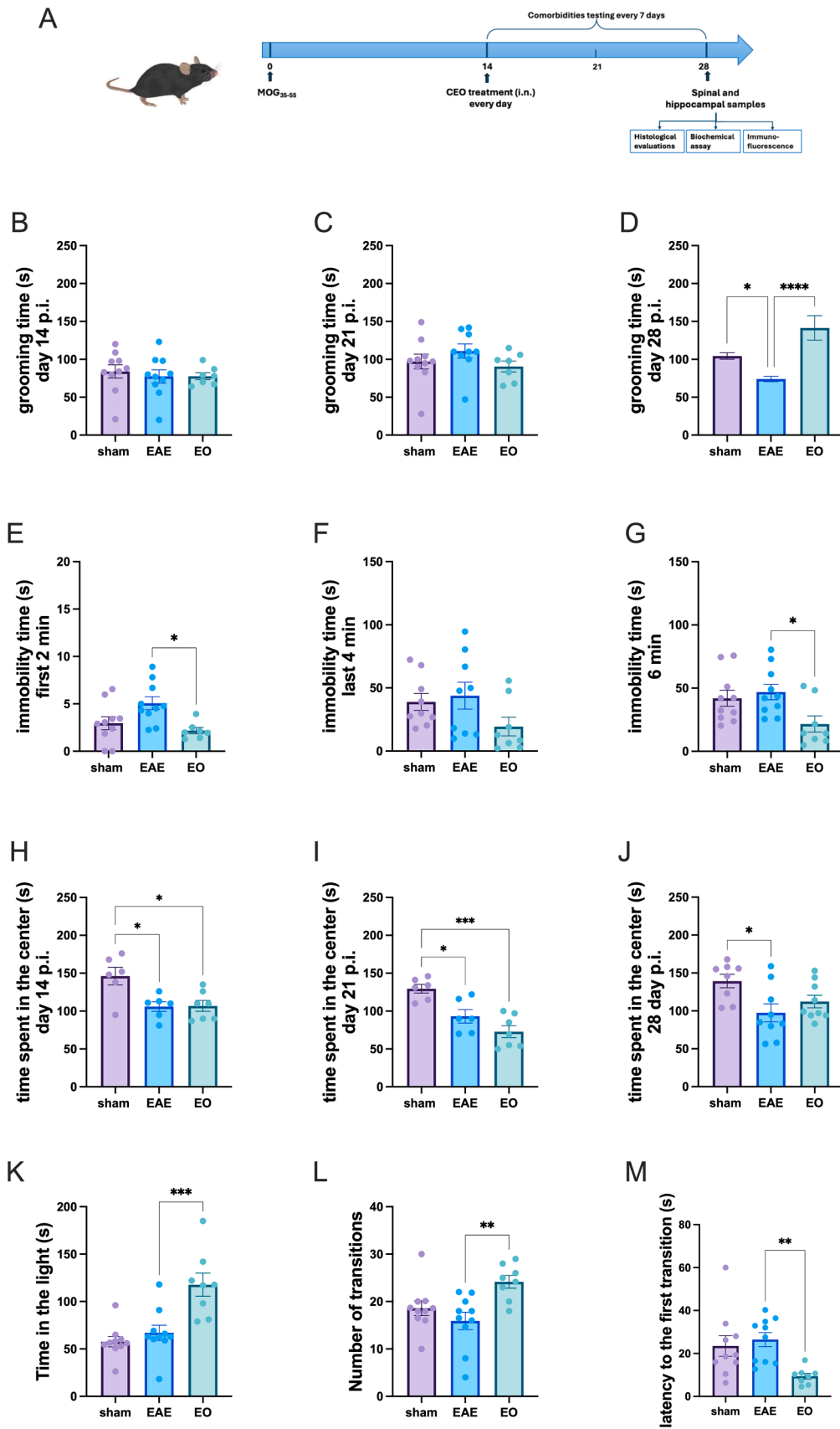
showed a very low level of CB2 protein in sham animals, while EAE mice showed an increased fluorescent staining prominently in the external laminae of the dorsal horn spinal cord, consistent with the observation of a CB2 overexpression in neuroinflammatory conditions (Grabon et al., 2023; Komorowska-Müller and Schmöle, 2021). CB2 immunostaining (Fig. 5O) and protein expression (Fig. 5P) were further increased by EO.

EO protects from hippocampal neuroinflammation and promotes microglia shift towards anti-inflammatory phenotype

The observation of spinal microglia shifts toward an anti-inflammatory phenotype by EO encouraged us to extend the investigation to the supraspinal areas to correlate the attenuation of neuroinflammation to the antidepressant-like and anxiolytic-like effect of the treatment. Hippocampal samples from EAE mice showed increased levels of IBA-1 (Fig. 6A) and CD11b (Fig. 6B) compared to sham mice, that were not significantly reduced by EO treatment. The calculation of the CD11b/IBA-1 ratio highlighted an increased value in EAE mice that

returned to basal sham levels after EO treatment (Fig. 6C). The expression of IL-10 (Fig. 6D) and IL-17 (Fig. 6E) were quantified indicating high levels of both cytokines in EAE hippocampal samples compared to sham. EO drastically increased IL-10 contents, while did not alter IL-17 levels. IL-17/IL-10 ratio values showed no differences between sham and EAE groups while a reduction of ratio value was produced by EO (Fig. 6F). Consistent with spinal results, the levels of CD4 (Fig. 6G) and FoxP3 (Fig. 6H) were increased, along with an increase of CD206, a marker of anti-inflammatory microglia (Fig. 6I), and CB2 receptors (Fig. 6J) in EAE. Levels of all markers were further potentiated by EO.

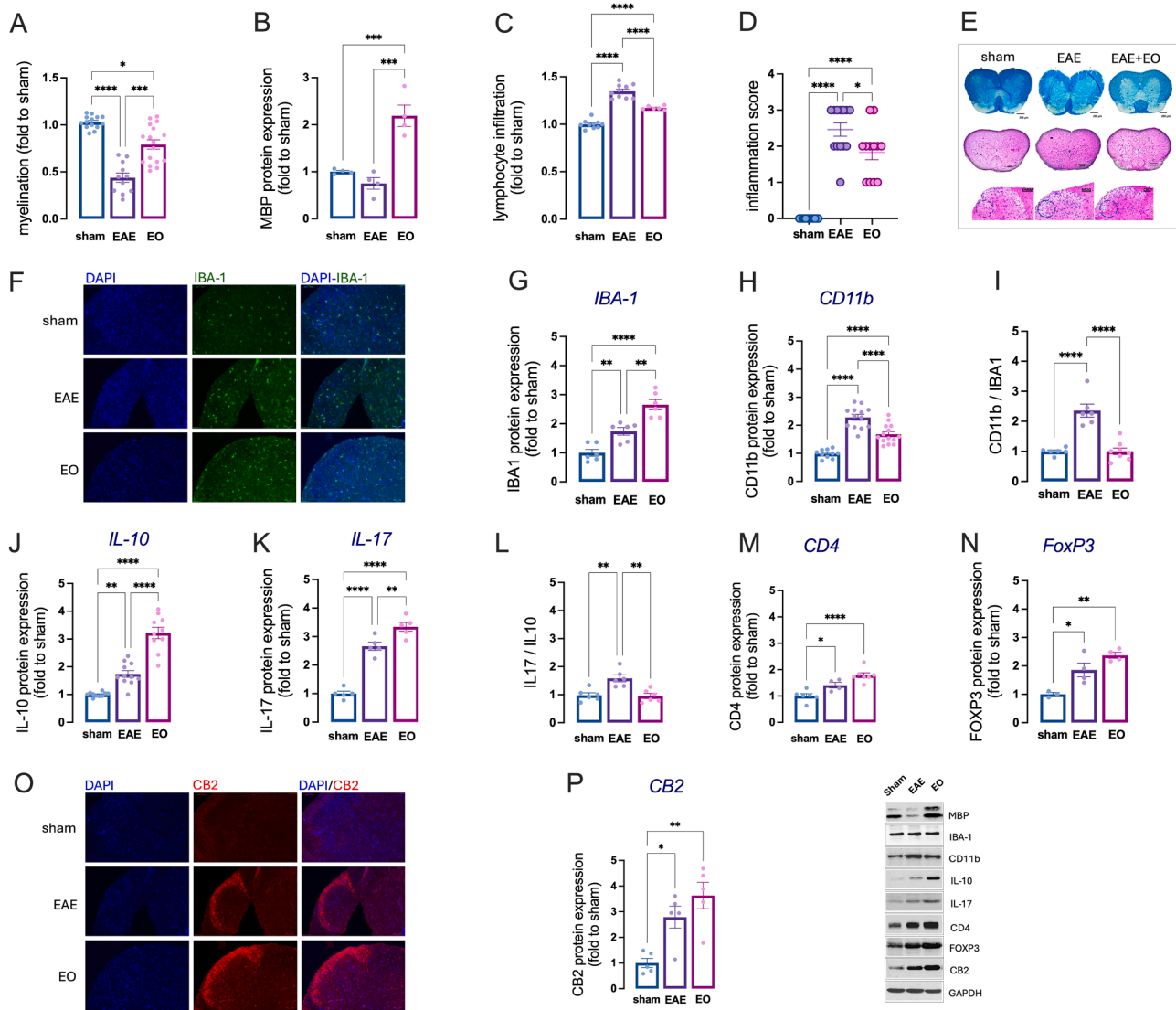
Finally, the expression of p-ERK (Fig. 6K) and p-CREB (Fig. 6L), involved both in neuroinflammation and in the modulation of memory and emotional processes (Albert-Gascó et al., 2020), were detected. Both markers were increased in the EAE hippocampal samples and EO returned protein expression to basal sham levels, further supporting a correlation between behavioral and biochemical evaluations.



(caption on next page)

Fig. 4. Antidepressant-like and anxiolytic-like activity of intranasal EO.

(A) Schematic representation of the experimental protocol. In the sucrose splash test (SST) EAE mice showed grooming times comparable to sham on 14 (B) and 21 (C) d.p.i., while it was reduced 28 dp.i. (D). Repeated administration of EO increased the grooming time 28 dp.i. In the tail suspension test (TST) EAE mice showed a trend toward increased immobility time in the first 2 min (E) and last 4 min (F) period of the test. EO decreased the immobility time values. The same effect was detected over the total 6-min period of the test (G). A reduction of the time spent in the center in the arena by EAE mice was observed during the open field (OF) test 14 (H), 21 (I) and 28 (J) d.p.i. No significant effect was produced by EO treatment. In the light-dark box (LDB) test EAE mice showed no variation in the time spent in the light chamber (K), in the number of transitions between the two chambers (L), and in the latency to the first transition (M) compared to sham mice. EO repeated administration increased the time in the light, the number of transitions and reduced the latency to the first transition. All groups tested included eleven animals. * $p < 0.05$; ** $p < 0.01$, *** $p < 0.001$, **** $p < 0.0001$.

**Fig. 5.** EO protects EAE mice from spinal demyelination and neuroinflammatory cell infiltration.

(A) Quantification analysis of Luxol Fast Blue (LFB) staining of spinal cord samples from sham, EAE and EO-treated EAE mice. (B) Increase of MBP expression by EO administration. EO reduced the lymphocyte infiltration (C) and the proinflammatory score (DE) compared to EAE mice. (EF) Representative images of LFB staining and Eosine & Hematoxylin (E&H) staining of spinal cord sections from sham, EAE and EO-treated EAE mice. Scale bar. 200 μm (low magnification), 50 μm (high magnification). * $p < 0.05$; ** $p < 0.01$, *** $p < 0.0001$. EO attenuation of neuroinflammation and microglia shift towards anti-inflammatory phenotype in the spinal cord. (F) Representative images of spinal cord section labeled with DAPI, Iba1 and merged from sham, EAE mice and EO-treated mice (Scale bar = 50 μm). Expression of Iba1 (GA), CD11b (HB) and CD11b/Iba1 ratio (IC) in spinal cord samples from sham, EAE and EAE-treated mice showing a reduction of the proinflammatory microglia following EO administration. (JE) (EAE mice showed a trend towards an increase of IL-10 protein expression that was robustly increased by EO. (F) Increase of FoxP3 expression in EAE mice that was further augmented by EO. (KG) EAE mice showed high levels of IL17 that were unmodified by EO administration. (LH) Increase of the IL17/IL10 ratio that was drastically reduced by EO. (F) Increase of CD4 (M) and FoxP3 (N) expression in EAE mice that was further augmented by EO. (O) Representative immunofluorescence micrographs of spinal cord section labeled with DAPI, CB2 and merged from sham, EAE mice and EO-treated mice (Scale bar = 50 μm). (PI) CB2 was significantly overexpressed by MOG35-55 immunization. EO treatment further increased CB2 protein levels. * $p < 0.05$; ** $p < 0.01$, *** $p < 0.001$, **** $p < 0.0001$.

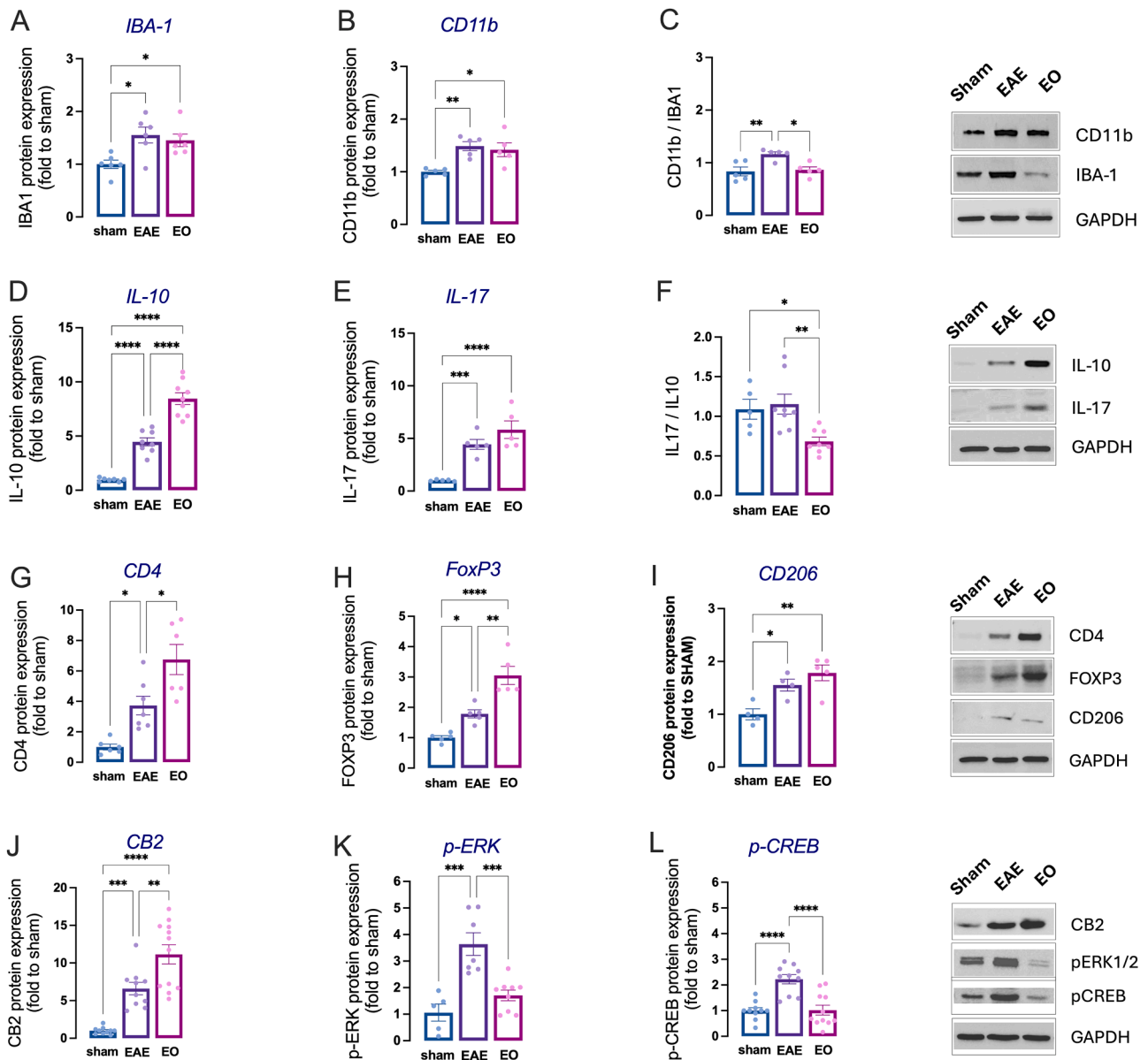
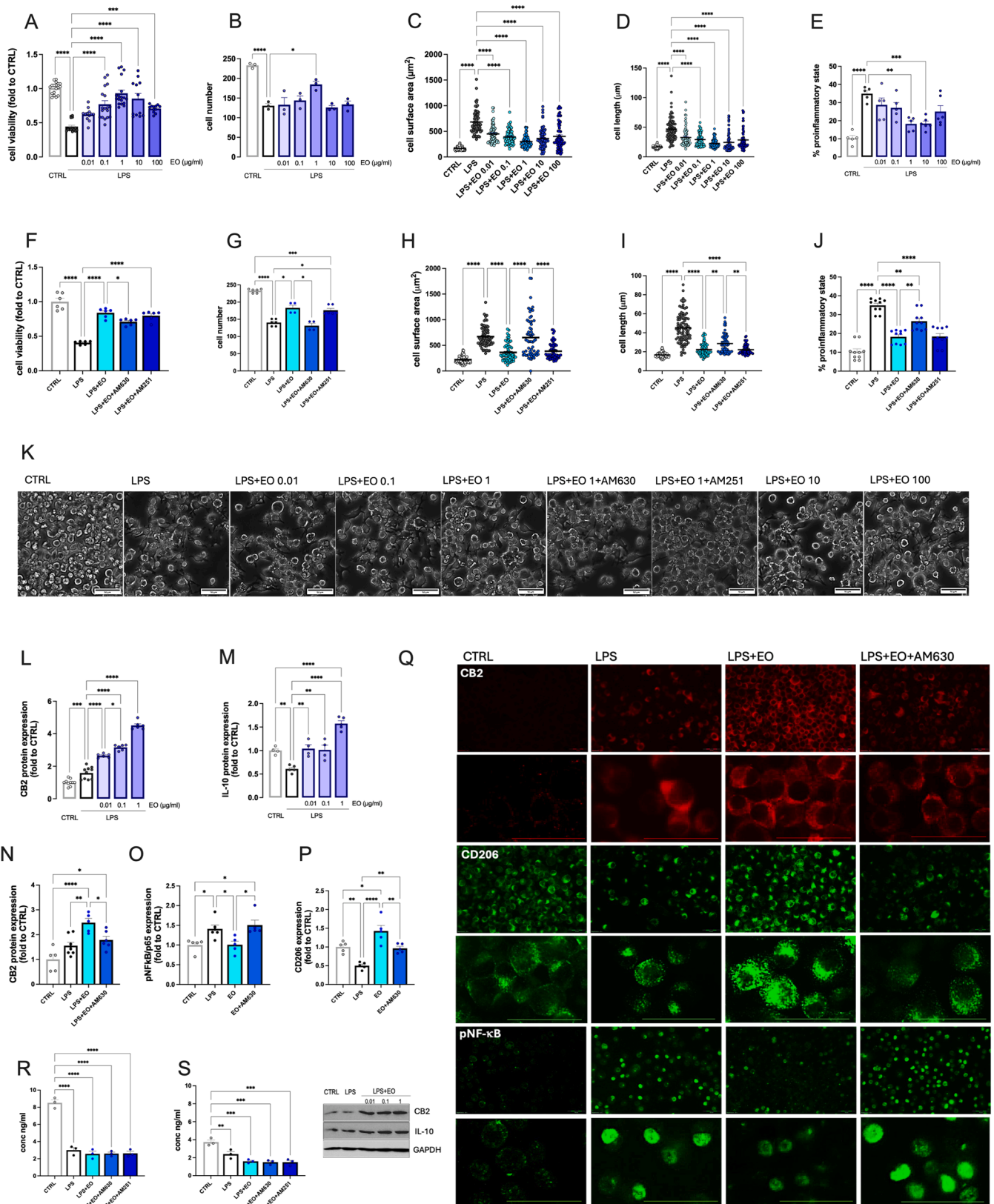


Fig. 6. Hippocampal neuroinflammation attenuation and microglia shift towards anti-inflammatory phenotype by EO. EAE hippocampal samples showed increased expression of Iba1(A) and CD11b (B) that remained unmodified following EO administration. (C) CD11b/Iba1 ratio showed an increased value in EAE that return to control levels in EO-treated mice. (D) EAE mice showed a trend towards an increase of IL-10 protein expression that was robustly increased by EO. (E) EAE mice showed high levels of IL17 that were unmodified by EO administration. (F) Increase of the IL17/IL10 ratio that was drastically reduced by EO. Increase of CD4 (G) and FoxP3 (H) expression in EAE mice that was further augmented by EO. (I) Protein expression of CD206, marker of anti-inflammatory microglia, was increased in both EAE and EO-treated mice. (JC) Overexpression of CB2 receptors in immunized mice that was further increased in the EO group. EO treatment further increased CB2 protein levels. EAE hippocampal samples showed increased phosphorylation of ERK (KA) and CREB (LB) proteins that returned to basal levels by EO treatment. (C) Overexpression of CB2 receptors in immunized mice that was further increased in the EO group. (D) Iba1 expression was increased in EAE mice and remained unmodified following EO administration. (D) Protein expression of CD206, marker of anti-inflammatory microglia, was increased in both EAE and EO-treated mice. (C) in spinal cord samples from sham, EAE and EAE-treated mice showing a reduction of the proinflammatory microglia following EO administration. (E) (EAE mice showed a trend towards an increase of IL-10 protein expression that was robustly increased by EO. (F) Increase of FoxP3 expression in EAE mice that was further augmented by EO. (G) EAE mice showed high levels of IL17 that was unmodified by EO administration. (H) Increase of the IL17/IL10 ratio that was drastically reduced by EO. (I) CB2 was significantly overexpressed by MOG35-55 immunization. EO treatment further increased CB2 protein levels. * $p < 0.05$; ** $p < 0.01$, *** $p < 0.001$, **** $p < 0.0001$.

EO attenuation of BV2 microglia cells proinflammatory phenotype

To assess the pivotal role of microglia in the mechanism of action of EO, a morphological analysis was conducted on BV2 cells exposed to LPS (250 ng/ml) for 24 h. The cell viability (Fig. 7A) and number (Fig. 7B) were drastically reduced (about 50–60% of control group) by LPS along with a progressive shift toward a microglia proinflammatory phenotype. The unstimulated BV2 cells are mainly found in the round phenotype

and, under LPS stimulation, the number of cells in the elongated phenotype significantly raised. A morphological analysis showed that LPS increased cell surface area (Fig. 7C) and diameter (Fig. 7D). Overall, the percentage of cells in the proinflammatory state was increased of about 3 times compared to control group (Fig. 7E). EO (0.01–100 $\mu\text{g/ml}$), produced a dose-dependent recover of reduced cell viability (Fig. 7A) and number (Fig. 7B) with a peak effect at 1 $\mu\text{g/ml}$. At higher doses the activity progressively reduced showing a bell-shaped trend.



(caption on next page)

Fig. 7. Effect of EO on neuroinflammation in LPS-stimulated BV2 cells. (A) Dose-response improvement by EO (0.01–100 µg/ml) of cell viability reduction induced by LPS stimulation (250 ng/ml for 24 h). (B) Protection by EO (0.01–1 µg/ml) of LPS-induced cell number decrease. Dose-dependent reduction by EO treatment of cell surface area (C), cell length (D) and number of BV2 cells in the proinflammatory state (E) after LPS exposure. Pretreatment with the CB2 antagonist AM630 (1 µM) prevented the EO effect on cell viability (F), total cell number (G), cell soma area (H), cell diameter (I) and percentage of cells in the proinflammatory state (J), while treatment with the CB1 antagonist AM251 (1 µM) was ineffective. (K) Representative images of CTRL, LPS-treated and EO-treated BV2 cells. Scale bar: 50 µm. (L) Dose-dependent increase of CB2 expression by EO (0.01, 0.1, 1 µg/ml). (M) Restoration to CTRL values (EO 0.01, 0.1 µg/ml) and increase (EO 1 µg/ml) of IL-10 protein levels reduced by LPS stimulation. (N) AM630 prevented the increase of CB2 receptors induced by EO 1 µg/ml. (O) Exposure to LPS increased the expression of p-NFκB, that was reduced to CTRL levels by EO (1 µg/ml). AM630 prevented the EO effect. (P) A reduction of CD206 content was detected in LPS-exposed cells that was largely increased by EO (1 µg/ml) through a CB2-mediated mechanism. LPS-stimulation reduced the extracellular levels of PEA (R) and 2-AG (S) that were not modified by EO. AM630 or AM251 treatment were ineffective. (Q) Low and high magnification representative images from immunofluorescence experiments from CTRL and LPS-stimulated BV2 cells in the absence (LPS) or in the presence of EO (LPS+EO) or EO and AM630 (LPS+EO+AM630) for CB2, CD206 and p-NFκB immunostaining. Scale bar: 50 µm. **p* < 0.05, ***p* < 0.01, ****p* < 0.001, *****p* < 0.0001.

Morphological analysis showed a dose-dependent reduction of morphological parameters by EO with a peak effect at 1 µg/ml, indicating a shift towards a resting phenotype.

EO promotes the shift of proinflammatory microglia cell phenotype through a CB2-mediated mechanism

To evaluate the involvement of the endocannabinoid system in the mechanism of action of EO, BV2 cells were pretreated with AM630, a CB2 antagonist, or AM251, a CB1 antagonist. AM630 selectively prevented the positive effect of EO on cell viability (Fig. 7F) and cell number (Fig. 7G) reduction. Consistently, AM630 attenuated the EO-induced reduction of proinflammatory cell morphology, as indicated by the increased cell surface area (Fig. 7H) and diameter (Fig. 7I) values, and by the higher percentage of cells in the proinflammatory state (Fig. 7J). Conversely, no effect was produced by AM251 (Fig. 7F–J).

To further assess the contribution of CB2-mediated effects in the EO activity, the correlation between a proinflammatory phenotype and the expression of CB2 receptors was investigated. Consistently with spinal and hippocampal tissue analysis, LPS-stimulated BV2 cells showed an increase in the CB2 (Fig. 7L) and IL-10 (Fig. 7M) protein expression that was dose-dependently increased by EO with a peak effect at 1 µg/ml (Fig. 7L). Furthermore, EO returned to basal levels the LPS-induced increased expression of p-NFκB (Fig. 7O) and largely restored the reduced expression of CD206 (Fig. 7P). These effects were prevented by AM630 (Fig. 7N,O,P). Immunofluorescence experiments further confirmed microglia shift toward an anti-inflammatory phenotype through a CB2-mediated mechanism (Fig. 7Q). Images showed a stretched and elongated morphology of microglia cells and a reduced cell number following LPS exposure and an increased CB2 receptor staining mainly located at cell prolongations. Following EO treatment, the cell number raised and a morphological shift toward a short-round phenotype was produced. A further increase in the CB2 immunostaining and restoration of CD206 levels was detected in EO-exposed cells. AM630 treatment prevented the EO effects. Finally, LPS-stimulated cells showed an increase immunostaining in the p-NFκB that was attenuated by EO. AM630 prevented the EO activity as illustrated by a p-NFκB immunostaining comparable to LPS-treated cells. The CB2-mediated mechanism was further supported by the selective antagonism of EO-induced antiallodynic activity of AM630 while AM251 was ineffective (Fig. S2).

Quantitative analysis of PEA and 2-AG released by microglia cells

The analytical method employed allowed for the selective and reliable quantification of both palmitoylethanolamide (PEA) and 2-arachidonoylglycerol (2-AG) in the cell culture medium. Despite attempts to measure other related endocannabinoids, such as oleoylethanolamide (OEA) and anandamide (AEA), their concentrations were consistently found to be below the limit of detection

(LOD). Quantification analysis showed that PEA (Fig. 7R) and to a lesser extent 2-AG (Fig. 7S) were markedly reduced by LPS stimulation. Treatment with EO (1 µg/ml) was devoid of any effect. Furthermore,

neither AM630 nor AM251 modified the endocannabinoid levels (Fig. 7R,S).

Discussion

The present study shows the efficacy of an essential oil from non-psychoactive *Cannabis sativa* L. to improve the overall symptomatology of EAE mice, including motor and algic symptoms and main comorbidities by promoting an anti-neuroinflammatory response through a CB2-mediated mechanism.

Repeated intranasal administration of EO attenuated cold allodynia, hot hyperalgesia, mechanical allodynia and motor disability, which represents the main symptoms of EAE mice, mirroring the main clinical symptoms in MS patients. Preclinical and clinical studies have demonstrated the efficacy and safety of medical cannabis and cannabis-based medications to alleviate spasticity and pain in MS or EAE, underscoring the therapeutic value of cannabinoids (Sirbu et al., 2023). From a pharmacological perspective, essential oils have traditionally been regarded mainly as modulators of cannabinoid-related effects through the so-called “entourage effect” (Koltai and Namdar, 2020) and remain less extensively characterized than cannabinoids. Nevertheless, antimicrobial properties have been described (Iseppi et al., 2019; Nissen et al., 2010; Zheljzakov et al., 2025), along with evidence of insecticidal and anti-inflammatory activities (Barbalace et al., 2023; Rossi et al., 2020) and emerging data suggest potential benefits in neurological disorders (Purushothaman and Krishnan, 2025). A recent study showed the efficacy of a Moroccan EO in a mouse model of trauma-induced peripheral neuropathy (Kaby et al., 2025) and similar results were reported for a Chinese EO in the paclitaxel-induced peripheral neuropathic pain model (Xu et al., 2024). In the context of MS, beneficial effects of hemp seed oil, a vegetable oil rich in fatty acids and devoid of terpenes, have been hypothesized (Al-Naqeb et al., 2023) However, to the best of our knowledge, no studies have yet reported analgesic or disability-improving effects in EAE models.

Anxiety and depression are the most common psychiatric comorbidities in MS patients (Rodrigues et al., 2023). Emotional alterations are also observed in EAE mice and, interestingly, the investigated EO attenuated these symptoms showing an antidepressant-like and anxiolytic-like activity. The effects of medical cannabis on mood disorders are complex, with conflicting efficacy reports (Sharpe et al., 2020). Research has focused on cannabinoids, while terpenes, the largest phytochemical class beyond cannabinoids, are poorly studied and their impact on mood alterations has not been investigated. Thus, our study represents the first evidence that a sesquiterpene-rich EO mitigates pain, motor symptoms and mood-related comorbidities in EAE.

Tissue analysis suggests that EO improved EAE symptomatology by attenuating CNS neuroinflammation and myelin damage by promoting a microglia-mediated anti-inflammatory response. Microglia play a critical role in all stages of MS by promoting neuroinflammatory and neurodegenerative processes (Hammond et al., 2024). EO restored the imbalanced CD11b/IBA-1 ratio to control values, indicating an attenuation of the microglia-mediated proinflammatory response. Given the central role of microglia and lymphocyte infiltration in the EAE/MS

onset and progression, modulating these cells is considered an essential target to control disease progression. MS immunopathology is primarily associated to myelin-reactive CD4⁺ Th, with a prominent role played by Th17 (producing IL-17) (Moser et al., 2020). In contrast, the anti-inflammatory population of T cells, such as Treg, results in inflammation resolution. Indeed, CD4⁺, FoxP3⁺ Tregs have an immune-modulating function by the release of the anti-inflammatory mediators IL-10 and TGF- β (Bar-Or and Li, 2021). EO restored the imbalanced IL-17/IL-10 ratio to levels detected in the sham group and, consistently, increased levels of FoxP3, allowing to hypothesize a polarization towards an inflammation resolving phenotype. Imbalance of Th and Treg has been hypothesized to play an essential role in the pathogenesis of MS through the expansion of auto-aggressive lymphocytes that finally leads to the myelin and axon damage (Lee, 2018). Several studies on EAE mice showed positive outcome by targeting Treg (Afzali et al., 2007; Jia et al., 2022), suggesting that down-regulation of pro-inflammatory Th17 cells and promotion of Treg responses might represent potential strategies to protect against the development of MS. Support for this hypothesis is found in approved disease-modifying drugs (i.e., IFN- β), which increased Treg cell count and this effect could explain the mechanism of their therapeutic efficacy (Duffy et al., 2019).

The endocannabinoid system modulates microglial activation in neuroinflammatory and neurodegenerative disease conditions mainly through CB2 receptor signaling, shifting gene expression from neuro-inflammatory to neuroprotective/homeostatic (Komorowska-Müller and Schmöle, 2021). Reversal of EO effects by the CB2 antagonist AM630 let hypothesized a CB2-mediated activity. These findings are consistent with previous observation reporting the involvement of CB2 receptors in the antiallodynic activity of a Moroccan EO in a peripheral neuropathy mouse model (Xu et al., 2024). At physiological conditions CB2 receptors have a very low level of expression. Conversely, during brain inflammatory processes, microglia become activated inducing upregulation of CB2 receptors as part of the immune response to maintain homeostasis (Grabon et al., 2024). EAE mice showed higher CB2 expression than sham mice. Interestingly, EO drastically elevated CB2 levels further supporting the hypothesis of a promotion of an anti-inflammatory response.

Mood disorders have been associated to microglia activation (Wang et al., 2022). Investigations into hippocampal samples from EAE mice showed an imbalanced CD11b/IBA-1 ratio that was restored by EO treatment at antidepressant-like and anxiolytic-like doses. Treatment also increased the expression of CD206, indicating a shift towards a microglia anti-inflammatory phenotype. Neuroinflammation and microglia activation in mood-related brain regions of MS patients play a key role in the development of anxiety and depression (Duffy et al., 2021). Consistently with findings from spinal cord tissue analysis, EO attenuated neuroinflammation, as indicated by the reduction of the IL-17/IL-10 ratio, and the raise of FoxP3 supported the hypothesis of a polarization toward a Treg-mediated response.

The anti-inflammatory properties of CB2 receptors are one of the main ways in which they affect mood (Bala et al., 2024). EAE increased the hippocampal expression of CB2 that was drastically elevated by EO. Experiments on LPS-stimulated BV2 microglia cells further defined the induction of a CB2-mediated microglia polarization by EO. In addition, a dose-dependent shift towards an anti-inflammatory morphology, the elevated levels of CD206 and IL-10 and the reduction of p-NF κ B suggested a polarization toward a microglia anti-inflammatory phenotype. All these events followed a selective AM630-sensitive mechanism. An indirect mechanism mediated by an increased release of antinociceptive and anti-inflammatory endocannabinoids, such as 2-AG and PEA, seems unlikely, as EO did not alter endocannabinoid levels. CB2 agonists are reported to be promising interventions for mood disorders (Hashiesh et al., 2021), indicating a CB2-mediated microglia polarization as a possible mechanism for the anxiolytic-like and antidepressant-like effects of EO.

The quantitative analysis of terpenes from EO identified BCP, α -humulene, and caryophyllene oxide as major constituents of the EO. Accumulating evidence has supported the intrinsic pharmacological activity of from *C. sativa* EO. Terpenes, in addition to the “entourage effect”, can exert biological activities independently of cannabinoids by acting on distinct molecular targets involved in nociceptive signalling and neuroinflammatory processes. Preclinical studies indicate that several terpenes display pleiotropic mechanisms of action, which may contribute to analgesic effects either autonomously or in combination with other bioactive constituents (Liktör-Busa et al., 2021). BCP is a CB2 agonist endowed with anti-inflammatory, analgesic and neuroprotective activities. Although efficacy of purified α -humulene in pain modulation has not been investigated, numerous studies on EOs and plant extracts containing this terpene provide evidence for an anti-inflammatory activity in the absence of direct interaction with the CB1 and CB2 receptors (Alfieri et al., 2025). The observed analgesic effects of EO may be mainly attributed to the CB2 stimulating properties of BCP, even though a contribution to the overall efficacy of EO by the anti-inflammatory activity of α -humulene cannot be excluded. *C. sativa* constituents in combination are well known to produce superior bioactivities than single molecules, producing the “entourage effect” (Koltai and Namdar, 2020). Thus, BCP, α -humulene and other terpenes present in EO may amplify their individual effects, leading to enhanced attenuation of pain hypersensitivity and to a more efficient neuroprotection. It cannot be excluded that the neuroprotective activity of EO, could depend, albeit partially, on the relatively high CBD content in the EO from this plant material.

Mono- and sesquiterpenes found in *C. sativa* EO have poor water solubility, high volatility and extensive first-pass metabolism that limited bioavailability (Alfieri et al., 2025), hindering their clinical use. Interestingly, we administered EO intranasally to foster brain penetration and limit metabolic systemic degradation. Intranasal administration offers a non-invasive route for drug delivery to the central nervous system that leads to rapid drug absorption and high bioavailability with an efficacy comparable to drugs delivered intrathecally (Borgonetti and Galeotti, 2021).

Conclusions

Present findings provide the first evidence that a sesquiterpene-rich EO obtained from non-psychoactive *C. sativa* mitigates EAE neurological symptoms, alleviating pain hypersensitivity, motor disability and mood-related comorbidities through a CB2-mediated anti-neuroinflammatory mechanism. The efficacy of EO appears to rely on the modulation of microglial activation and the restoration of immune balance, promoting a shift toward a neuroprotective, Treg-associated anti-inflammatory phenotype both at spinal and supraspinal levels. These findings expand the current pharmacological landscape of cannabis-derived products beyond cannabinoids, highlighting terpenes as active contributors in the EAE model. From a translational perspective, the intranasal delivery of EO represents a promising strategy to overcome the pharmacokinetic limitations of volatile terpenes and to selectively target central neuro-inflammatory processes. Future studies should aim to dissect the contribution of individual terpenes and their synergistic interactions, to evaluate EO effects in combination with approved disease-modifying therapies, and to explore efficacy as remyelinating agent. Moreover, investigation of EO activity in additional models of neuroinflammation and mood disorders, as well as pharmacokinetic and formulation studies, will be essential to support its development as a novel, non-psychoactive, multi-target therapeutic approach for MS and related neuroinflammatory conditions.

Funding

This work was supported by the Italian Ministry of the University and Research (MUR) – PRIN2022 project (CUP: B53D23020140006).

Ethics approval and consent to participate

The experimental protocol was approved by the Institution's Animal Care and Research Ethics Committee (University of Florence, Italy), under license from the Italian Department of Health (336/2022-PR). Mice were treated in accordance with the relevant European Union (Directive, 2010/63/EU) and international regulations. All studies involving animals are reported in accordance with the ARRIVE guidelines (McGrath and Lilley, 2015). All effort was taken to minimize the number of animals used and their suffering.

Availability of data and materials

All original data are available upon request.

CRediT authorship contribution statement

Giacomina Videtta: Investigation, Formal analysis. **Chiara Sasia:** Investigation, Formal analysis. **Sofia Quadrino:** Investigation, Formal analysis. **Virginia Brighenti:** Investigation, Data curation. **Laura Bertarini:** Investigation. **Clarissa Caroli:** Investigation. **Claudia Mugnaini:** Writing – review & editing. **Federica Pellati:** Writing – review & editing, Conceptualization, Writing – original draft, Supervision. **Nicoletta Galeotti:** Writing – review & editing, Writing – original draft, Supervision, Funding acquisition, Conceptualization.

Declaration of competing interest

The authors declare that they have no known competing financial interests or personal relationships that could have appeared to influence the work reported in this paper.

Supplementary materials

Supplementary material associated with this article can be found, in the online version, at [doi:10.1016/j.phymed.2026.158068](https://doi.org/10.1016/j.phymed.2026.158068).

References

- Adams, T.B., Gavin, C.L., McGowen, M.M., Waddell, W.J., Cohen, S.M., Feron, V.J., Marnett, L.J., Munro, I.C., Portoghese, P.S., Rietjens, I.M.C.M., Smith, R.L., 2011. The FEMA GRAS assessment of aliphatic and aromatic terpene hydrocarbons used as flavor ingredients. *Food Chem. Toxicol.* 49, 2471–2494. <https://doi.org/10.1016/j.fct.2011.06.011>.
- Afzali, B., Lombardi, G., Lechler, R.I., Lord, G.M., 2007. The role of T helper 17 (Th17) and regulatory T cells (Treg) in human organ transplantation and autoimmune disease. *Clin. Exp. Immunol.* 148, 32–46. <https://doi.org/10.1111/J.1365-2249.2007.03356.X>.
- Albert-Gascó, H., Ros-Bernal, F., Castillo-Gómez, E., Olucha-Bordonau, F.E., 2020. Map/erk signaling in developing cognitive and emotional function and its effect on pathological and neurodegenerative processes. *Int. J. Mol. Sci.* 21, 1–29. <https://doi.org/10.3390/IJMS21124471>.
- Alfieri, A., Di Franco, S., Maffei, V., Sansone, P., Pace, M.C., Passavanti, M.B., Fiore, M., 2025. Phytochemical modulators of nociception: a review of cannabis terpenes in chronic pain syndromes. *Pharmaceuticals (Basel)* 18, 1100. <https://doi.org/10.3390/PHI18081100>.
- Al-Naqeb, G., Kalmouztidou, A., De Giuseppe, R., Cena, H., 2023. Beneficial effects of plant oils supplementation on multiple sclerosis: a comprehensive review of clinical and experimental studies. *Nutrients* 15. <https://doi.org/10.3390/NU15224827>.
- Appendino, G., Chianese, G., Tagliatela-Scafati, O., 2011. Cannabinoids: occurrence and medicinal chemistry. *Curr. Med. Chem.* 18, 1085–1099. <https://doi.org/10.2174/092986711794940888>.
- Bala, K., Porel, P., Aran, K.R., 2024. Emerging roles of cannabinoid receptor CB2 receptor in the central nervous system: therapeutic target for CNS disorders. *Psychopharmacol. (Berl)* 241, 1939–1954. <https://doi.org/10.1007/S00213-024-06683-W>.
- Barbalace, M.C., Freschi, M., Rinaldi, I., Mazzara, E., Maraldi, T., Malaguti, M., Prata, C., Maggi, F., Petrelli, R., Hrelia, S., Angeloni, C., 2023. Identification of anti-neuroinflammatory bioactive compounds in essential oils and aqueous distillation residues obtained from commercial varieties of cannabis sativa L. *Int. J. Mol. Sci.* 24. <https://doi.org/10.3390/IJMS242316601>.
- Bar-Or, A., Li, R., 2021. Cellular immunology of relapsing multiple sclerosis: interactions, checks, and balances. *Lancet Neurol.* 20, 470–483. [https://doi.org/10.1016/S1474-4422\(21\)00063-6](https://doi.org/10.1016/S1474-4422(21)00063-6).
- Borgonetti, V., Galeotti, N., 2023a. Posttranscriptional regulation of gene expression participates in the myelin restoration in mouse models of multiple sclerosis: antisense modulation of HuR and HuD ELAV RNA binding protein. *Mol. Neurobiol.* 60, 2661–2677. <https://doi.org/10.1007/s12035-023-03236-8>.
- Borgonetti, V., Galeotti, N., 2023b. Microglia senescence is related to neuropathic pain-associated comorbidities in the spared nerve injury model. *Pain.* 164, 1106–1117. <https://doi.org/10.1097/J.PAIN.0000000000002807>.
- Borgonetti, V., Galeotti, N., 2021. Intranasal delivery of an antisense oligonucleotide to the RNA-binding protein HuR relieves nerve injury-induced neuropathic pain. *Pain.* 162, 1500–1510. <https://doi.org/10.1097/j.pain.0000000000002154>.
- Brighenti, V., Pellati, F., Steinbach, M., Maran, D., Benvenuti, S., 2017. Development of a new extraction technique and HPLC method for the analysis of non-psychoactive cannabinoids in fibre-type cannabis sativa L. (hemp). *J. Pharm. Biomed. Anal.* 143, 228–236. <https://doi.org/10.1016/j.jpba.2017.05.049>.
- Duffy, S.S., Hayes, J.P., Fiore, N.T., Moalem-Taylor, G., 2021. The cannabinoid system and microglia in health and disease. *Neuropharmacology.* 190. <https://doi.org/10.1016/J.NEUROPHARM.2021.108555>.
- Duffy, S.S., Keating, B.A., Moalem-Taylor, G., 2019. Adoptive transfer of regulatory T cells as a promising immunotherapy for the treatment of multiple sclerosis. *Front. Neurosci.* 13. <https://doi.org/10.3389/FNINS.2019.01107>.
- García-Valverde, M.T., Sánchez-Carnerero Callado, C., Díaz-Liñán, M.C., Sánchez de Medina, V., Hidalgo-García, J., Nadal, X., Hanus, L., Ferreira-Vera, C., 2022. Effect of temperature in the degradation of cannabinoids: from a brief residence in the gas chromatography inlet port to a longer period in thermal treatments. *Front. Chem.* 10. <https://doi.org/10.3389/FCHEM.2022.1038729>.
- Gonzalez-Lorenzo, M., Ridley, B., Minozzi, S., Del Giovane, C., Peryer, G., Piggott, T., Foschi, M., Filippini, G., Tramacere, I., Baldin, E., Nonino, F., 2024. Immunomodulators and immunosuppressants for relapsing-remitting multiple sclerosis: a network meta-analysis. *Cochrane Database of Systematic Rev.* 2024. <https://doi.org/10.1002/14651858.CD011381.PUB3>.
- Grabon, W., Rheims, S., Smith, J., Bodenec, J., Belmeuguenai, A., Bezin, L., 2023. CB2 receptor in the CNS: from immune and neuronal modulation to behavior. *Neurosci. Biobehav. Rev.* 150. <https://doi.org/10.1016/J.NEUBIOREV.2023.105226>.
- Grabon, W., Ruiz, A., Gasm, N., Degletagne, C., Georges, B., Belmeuguenai, A., Bodenec, J., Rheims, S., Marcy, G., Bezin, L., 2024. CB2 expression in mouse brain: from mapping to regulation in microglia under inflammatory conditions. *J. Neuroinflammation.* 21. <https://doi.org/10.1186/S12974-024-03202-8>.
- Guerrero, B.L., Sicotte, N.L., 2020. Microglia in multiple sclerosis: friend or foe? *Front. Immunol.* 11. <https://doi.org/10.3389/FIMMU.2020.00374>.
- Hammond, B.P., Panda, S.P., Kaushik, D.K., Plemel, J.R., 2024. Microglia and multiple sclerosis. *Adv. Neurobiol.* 37, 445–456. https://doi.org/10.1007/978-3-031-55529-9_25.
- Hashiesh, H.M., Jha, N.K., Sharma, C., Gupta, P.K., Jha, S.K., Patil, C.R., Goyal, S.N., Ojha, S.K., 2021. Pharmacological potential of JWH133, a cannabinoid type 2 receptor agonist in neurodegenerative, neurodevelopmental and neuropsychiatric diseases. *Eur. J. Pharmacol.* 909. <https://doi.org/10.1016/j.ejphar.2021.174398>.
- Healy, L.M., Stratton, J.A., Kuhlmann, T., Antel, J., 2022. The role of glial cells in multiple sclerosis disease progression. *Nat. Rev. Neurol.* 18, 237–248. <https://doi.org/10.1038/S41582-022-00624-X>.
- Iseppi, R., Brighenti, V., Licata, M., Lambertini, A., Sabia, C., Messi, P., Pellati, F., Benvenuti, S., 2019. Chemical characterization and evaluation of the antibacterial activity of essential oils from fibre-type cannabis sativa L. (Hemp). *Molecules.* 24. <https://doi.org/10.3390/MOLECULES24122302>.
- Jakimovski, D., Bittner, S., Zivadnov, R., Morrow, S.A., Benedict, R.H., Zipp, F., Weinstock-Guttman, B., 2024. Multiple sclerosis. *The Lancet* 403, 183–202. [https://doi.org/10.1016/S0140-6736\(23\)01473-3](https://doi.org/10.1016/S0140-6736(23)01473-3).
- Janatová, A., Doskokčil, I., Božik, M., Franková, A., Tlustoš, P., Klouček, P., 2022. The chemical composition of ethanolic extracts from six genotypes of medical cannabis (*Cannabis sativa* L.) and their selective cytotoxic activity. *Chem. Biol. Interact.* 353. <https://doi.org/10.1016/j.cbi.2022.109800>.
- Jia, Z., Liu, J., Li, B., Yi, L., Wu, Y., Xing, J., Wang, L., Wang, J., Guo, L., 2022. Exosomes with FOXP3 from gene-modified dendritic cells ameliorate the development of EAE by regulating the balance of Th/treg. *Int. J. Med. Sci.* 19, 1265–1274. <https://doi.org/10.7150/IJMS.72655>.
- Jin, D., Henry, P., Shan, J., Chen, J., 2021. Identification of chemotypic markers in three chemotype categories of cannabis using secondary metabolites profiled in inflorescences, leaves, stem bark, and roots. *Front. Plant Sci.* 12. <https://doi.org/10.3389/FPLS.2021.699530>.
- Jones, É., Vlachou, S., 2020. A critical review of the role of the cannabinoid compounds Δ9-tetrahydrocannabinol (Δ9-THC) and cannabidiol (CBD) and their combination in Multiple sclerosis treatment. *Molecules.* 25. <https://doi.org/10.3390/MOLECULES25214930>.
- Joy, N., Jackson, D., Coolong, T., 2025. A validated GC-MS method for major terpenes quantification in hydrodistilled cannabis sativa essential oil. *Phytochem. Anal.* 36, 2362–2373. <https://doi.org/10.1002/PCA.3526>.
- Kabdy, H., Abdelmounaim, B., Aitbaba, A., Hajar, A., Yasmine, J., Oufquir, S., Agouram, F., Laadraoui, J., Aboufatima, R., Belbachir, A., Garzoli, S., Chait, A., 2025. Moroccan cannabis sativa essential oil attenuates peripheral neuropathic pain induced by chronic sciatic nerve constriction injury in mice. *J. Ethnopharmacol.* 343. <https://doi.org/10.1016/j.jep.2025.119486>.
- KnocheImann, H.M., Dwyer, C.J., Bailey, S.R., Amaya, S.M., Elston, D.M., Mazza-McCrann, J.M., Paulos, C.M., 2018. When worlds collide: th17 and treg cells in cancer and autoimmunity. *Cell Mol. Immunol.* 15, 458–469. <https://doi.org/10.1038/S41423-018-0004-4>.

- Koltai, H., Namdar, D., 2020. Cannabis phytomolecule "entourage": from domestication to medical use. *Trends. Plant Sci.* 25, 976–984. <https://doi.org/10.1016/J.TPLANTS.2020.04.007>.
- Komorowska-Müller, J.A., Schmöle, A.C., 2021. CB2 receptor in microglia: the guardian of self-control. *Int. J. Mol. Sci.* 22, 1–27. <https://doi.org/10.3390/IJMS22010019>.
- Landrigan, J., Bessenyei, K., Leitner, D., Yakovenko, I., Fisk, J.D., Prentice, J.L., 2022. A systematic review of the effects of cannabis on cognition in people with multiple sclerosis. *Mult. Scler. Relat. Disord.* 57. <https://doi.org/10.1016/j.msard.2021.103338>.
- LaVigne, J.E., Hecksel, R., Keresztes, A., Streicher, J.M., 2021. Cannabis sativa terpenes are cannabimimetic and selectively enhance cannabinoid activity. *Sci. Rep.* 11. <https://doi.org/10.1038/S41598-021-87740-8>.
- Lee, G.R., 2018. The balance of Th17 versus treg cells in autoimmunity. *Int. J. Mol. Sci.* 19. <https://doi.org/10.3390/IJMS19030730>.
- Liktor-Busa, E., Keresztes, A., Lavigne, J., Streicher, J.M., Largent-Milnes, T.M., 2021. Analgesic potential of terpenes derived from cannabis sativa. *Pharmacol. Rev.* 73, 1270–1297. <https://doi.org/10.1124/pharmrev.120.000046>.
- Longoria, V., Parcel, H., Toma, B., Minhas, A., Zeine, R., 2022. Neurological benefits, clinical challenges, and neuropathologic promise of medical Marijuana: a systematic review of cannabinoid effects in multiple sclerosis and experimental models of demyelination. *Biomedicine.* 10. <https://doi.org/10.3390/BIOMEDICINES10030539>.
- Marini, E., Magi, G., Ferretti, G., Bacchetti, T., Giuliani, A., Pugnali, A., Ripponi, M.R., Facinelli, B., 2018. Attenuation of *Listeria monocytogenes* virulence by cannabis sativa L. Essential Oil. *Front. Cell. Infect. Microbiol.* 8. <https://doi.org/10.3389/FCIMB.2018.00293>.
- McGinley, M.P., Goldschmidt, C.H., Rae-Grant, A.D., 2021. Diagnosis and treatment of multiple sclerosis: a review. *JAMA - Journal of the American Medical Association* 325, 765–779. <https://doi.org/10.1001/JAMA.2020.26858>.
- McGrath, J.C., Lilley, E., 2015. Implementing guidelines on reporting research using animals (ARRIVE etc.): new requirements for publication in BJP. *Br. J. Pharmacol.* <https://doi.org/10.1111/bph.12955>.
- Micalizzi, G., Alibrando, F., Vento, F., Trovato, E., Zoccali, M., Guarnaccia, P., Dugo, P., Mondello, L., 2021. Development of a novel microwave distillation technique for the isolation of cannabis sativa L. Essential oil and gas chromatography analyses for the comprehensive characterization of terpenes and terpenoids, including their enantiomeric distribution. *Molecules.* 26. <https://doi.org/10.3390/MOLECULES26061588>.
- Moser, T., Akgün, K., Proschmann, U., Sellner, J., Ziemssen, T., 2020. The role of TH17 cells in multiple sclerosis: therapeutic implications. *Autoimmun. Rev.* 19. <https://doi.org/10.1016/j.autrev.2020.102647>.
- Motulsky, H.J., Brown, R.E., 2006. Detecting outliers when fitting data with nonlinear regression - a new method based on robust nonlinear regression and the false discovery rate. *BMC. Bioinformatics.* 7. <https://doi.org/10.1186/1471-2105-7-123>.
- Nissen, L., Zatta, A., Stefanini, I., Grandi, S., Sgorbati, B., Biavati, B., Monti, A., 2010. Characterization and antimicrobial activity of essential oils of industrial hemp varieties (*Cannabis sativa* L.). *Fitoterapia* 81, 413–419. <https://doi.org/10.1016/J.FITOTE.2009.11.010>.
- Odieka, A.E., Obuzor, G.U., Oyedeji, O.O., Gondwe, M., Hosu, Y.S., Oyedeji, A.O., 2022. The Medicinal Natural Products of *Cannabis sativa* Linn.: a review. *Molecules.* 27, 27. <https://doi.org/10.3390/MOLECULES27051689>, 2022.
- Pellati, F., Brighenti, V., Sperlea, J., Marchetti, L., Bertelli, D., Benvenuti, S., 2018. New methods for the comprehensive analysis of bioactive compounds in cannabis sativa L. (*hemp*). *Molecules.* 23. <https://doi.org/10.3390/MOLECULES23102639>.
- Pieracci, Y., Ascrizzi, R., Terreni, V., Pistelli, L., Flamini, G., Bassolino, L., Fulvio, F., Montanari, M., Paris, R., 2021. Essential oil of cannabis sativa L: comparison of yield and chemical composition of 11 hemp genotypes. *Molecules.* 26. <https://doi.org/10.3390/MOLECULES26134080>.
- Purushothaman, A., Krishnan, A., 2025. Unveiling neurological benefits: a review of hemp leaf, flower, seed oil extract, and their phytochemical properties in neurological disorders. *Cannabis. Cannabinoid. Res.* <https://doi.org/10.1177/25785125251410822/FORMAT/EPUB>.
- Radwan, M.M., Chandra, S., Gul, S., Elsohly, M.A., 2021. Cannabinoids, phenolics, terpenes and alkaloids of Cannabis. *Molecules.* 26. <https://doi.org/10.3390/MOLECULES26092774>.
- Ramaglia, V., Rojas, O., Naouar, I., Gommerman, J.L., 2021. The ins and outs of Central nervous system inflammation mdash lessons learned from multiple sclerosis. *Annu. Rev. Immunol.* 39, 199–226. <https://doi.org/10.1146/ANNUREV-IMMUNOL-093019-124155>.
- Riederer, F., 2017. Ocrelizumab versus placebo in primary progressive multiple sclerosis. *Journal für Neurologie, Neurochirurgie und Psychiatrie* 18, 30–31. <https://doi.org/10.1056/NEJM0A1606468>.
- Rodrigues, P., da Silva, B., Trevisan, G., 2023. A systematic review and meta-analysis of neuropathic pain in multiple sclerosis: prevalence, clinical types, sex dimorphism, and increased depression and anxiety symptoms. *Neurosci. Biobehav. Rev.* 154. <https://doi.org/10.1016/j.neubiorev.2023.105401>.
- Rossi, P., Cappelli, A., Marinelli, O., Valzano, M., Pavoni, L., Bonacucina, G., Petrelli, R., Pompei, P., Mazzara, E., Ricci, I., Maggi, F., Nabissi, M., 2020. Mosquitocidal and anti-inflammatory properties of the essential oils obtained from monoecious, male, and female inflorescences of hemp (*Cannabis sativa* L.) and their encapsulation in nanoemulsions. *Molecules.* 25. <https://doi.org/10.3390/MOLECULES25153451>.
- Sharpe, L., Sinclair, J., Kramer, A., De Manincor, M., Sarris, J., 2020. Cannabis, a cause for anxiety? A critical appraisal of the anxiogenic and anxiolytic properties. *J. Transl. Med.* 18. <https://doi.org/10.1186/S12967-020-02518-2>.
- Sirbu, C.A., Georgescu, R., Pleşa, F.C., Paunescu, A., Marilena Țanțu, M., Nicolae, A.C., Caloianu, I., Mitrica, M., 2023. Cannabis and cannabinoids in multiple sclerosis: from experimental models to clinical practice-A review. *Am. J. Ther.* 30, E220–E231. <https://doi.org/10.1097/MJT.0000000000001568>.
- Vuerich, M., Ferfua, C., Zuliani, F., Piani, B., Sepulcri, A., Baldini, M., 2019. Yield and quality of essential oils in hemp varieties in different environments. *Agronomy* 9, 9. <https://doi.org/10.3390/AGRONOMY9070356>, 2019.
- Wang, H., He, Y., Sun, Z., Ren, S., Liu, M., Wang, G., Yang, J., 2022. Microglia in depression: an overview of microglia in the pathogenesis and treatment of depression. *J. Neuroinflammation.* 19. <https://doi.org/10.1186/S12974-022-02492-0>.
- Xu, Y., Luo, J., Guo, Y., Zhou, J., Shen, L., Gu, F., Shi, C., Yao, L., Hua, M., 2024. Chemical compounds, anti-tumor and anti-neuropathic pain effect of hemp essential oil in vivo. *Fitoterapia* 177, 106092. <https://doi.org/10.1016/J.FITOTE.2024.106092>.
- Zheljazzkov, V.D., Semerdjieva, I., Sikora, V., Dincheva, I., Kačaniová, M., 2025. Essential oils (EOs) composition and antimicrobial activities of novel cannabis sativa L (*Hemp*) selections from Serbia. *Ind. Crops. Prod.* 235, 121615. <https://doi.org/10.1016/J.IJNCROP.2025.121615>.